Supplementary Information

A data-driven approach to predicting band gap, excitation, and emission energies for Eu^{2+}-activated phosphors

Chaewon Park[a,‡], Jin-Woong Lee[a,‡], Minseuk Kim[a,‡], Byung Do Lee, Satendra Pal Singh,[a] Woon Bae Park[b,*], and Kee-Sun Sohn[a,*]

[a]Nanotechnology & Advanced Materials Engineering, Sejong University, 209 Neungdong-ro, Gwangjin-gu, Seoul, 143-747, South Korea

[b]Department of Printed Electronics, Sunchon National University, 291-19 Jungang-ro, Sunchon, Chonnam, 540-742, South Korea

[‡]These authors contributed equally

Corresponding authors: kssohn@sejong.ac.kr, wbpark@scnu.ac.kr

List of Contents

Fig. S1 The training, validation and hold-out dataset test results for PEW prediction in terms of (a,e) MSE and (b,f) R^2 for 9 cross validation and 8-fold cross validation with a holdout dataset test, (c,g) the over-fitting index defined as Training_MSE/Validation_MSE and Validation_R^2/Training_R^2, and (d,f) the over-fitting index defined as Training_MSE/Test_MSE and Test_R^2/Training_R^2. (a)~(d) stand for EBEW prediction model results and (e)~(h) for E_g results.

Fig. S2 Plots of predicted vs. experimental (a) PEW, (b) EBEW, and (c) E_g for training and validation datasets for 9-fold cross validation.

Fig. S3 Plots of ML-predicted vs. experimental (a) PEW, (b) EBEW, and (c) E_g for every ML algorithm for leave-one-out cross-validation with no holdout test dataset.

Fig. S4 The surrogate ML model regression results. Plots of the ML-predicted vs. experimental (a) PEW, (b) EBEW, and (c) E_g for every ML algorithm for 8-fold cross-validation with a holdout dataset test.

Table S1. All the attempted hyper-parameter sets for each algorithm, which is a search space mesh to be screened to discover the best set. The finally selected set is highlighted in bold font.

Ridge	lasso	LARS	ENR	
alpha	alpha	alpha	l1_ratio	alpha
	0.00001			
	0.00005			
0.001	0.0001			**0.001**
0.005	0.0005	0.0001		0.005
0.01	**0.001**	**0.001**	0.3	0.01
0.05	0.005	0.01	0.5	0.05
0.1	0.01	0.1	**0.7**	0.1
0.5	0.05	1		0.5
1	0.1			1
	0.5			
	1			

KRR		BRR	ARD			
kernel	alpha	tol	alpha_1	alpha_2	lambda_1	lambda_2
linear	0.001	**0.00001**				
poly	**0.01**	0.0001	1e-04	**1e-04**	**1e-04**	1e-04
rbf	0.1	0.001	1e-06	1e-06	1e-06	**1e-06**
sigmoid	1	0.01	**1e-08**	1e-08	1e-08	1e-08
matern		0.1				

RF			Ada Boost		
max_features	n_estimators	max_depth	loss	learning_rate	n_estimators
auto	50	5	exponential	0.001	**50**
log2	**100**	**10**	linear	**0.01**	100
sqrt	150	15	**square**	0.1	150
				1	

Gradient Boost			
loss	subsample	learning_rate	n_estimators
ls **lad** huber quantile	0.4 **0.7** 1	0.001 0.01 **0.1** 1	50 **100** 150

XG Boost			SVR	
subsample	learning_rate	max_depth	kernel	c
0.4 0.7 1	0.001 0.01 **0.1** 1	**4** 6 8	**linear** poly rbf sigmoid matern	0.001 0.01 0.1 **1**

KNN			PLS	GPR			
weights	n_neighbors	p	n_components	kernel	length_scale	nu	alpha
uniform **distance**	**3** 5 7 11 13	**1** 2	**1**	**matern**	1 **10** 100	**0.5** 1.5 2.5	1e-01 1e-04 1e-07 **1e-10**

Table S2. Details of the validation MSE and R^2 values for all the hyper-parameter sets (9-fold cross-validation with no holdout dataset test). The hyper parameter screening process is based on the PEW prediction model since it is a baseline that showed worse fitting quality in comparison to both the EBEW and E_g prediction models.

Ridge

hyper parameter	Regression result			
alpha	MSE (training)	R^2 (training)	MSE (validation)	R^2 (validation)
0.001	0.011135689	0.803128148	0.025556201	0.482478192
0.005	0.011072263	0.80444746	0.026817088	0.496703389
0.01	0.01109431	0.804057755	0.026098383	0.511561206
0.05	0.011296572	0.80046335	0.023830077	0.5560478
0.1	0.011545196	0.79605114	0.022758552	0.577783215
0.5	**0.01335052**	**0.764062538**	**0.021242255**	**0.617683994**
1	0.015162412	0.732088215	0.02182785	0.611494981

Lasso

hyper parameter	Regression result			
alpha	MSE (training)	R^2 (training)	MSE (validation)	R^2 (validation)
0.00001	0.011136036	0.803122059	0.025572297	0.482480705
0.00005	0.011084831	0.80422242	0.026574723	0.499839942
0.0001	0.011149394	0.803083162	0.025495275	0.523081344
0.0005	0.01231518	0.78231046	0.022151031	0.592592334
0.001	**0.013409026**	**0.763006584**	**0.021753577**	**0.603333314**
0.005	0.021266607	0.623791844	0.025226279	0.56129263
0.01	0.029494771	0.478999474	0.031745084	0.441370422
0.05	0.056602334	0	0.057069362	-0.029931033
0.1	0.056602334	0	0.057069362	-0.029931033
0.5	0.056602334	0	0.057069362	-0.029931033
1	0.056602334	0	0.057069362	-0.029931033

LARS

hyper parameter	Regression result			
alpha	MSE (training)	R^2 (training)	MSE (validation)	R^2 (validation)
0.0001	0.011311751	0.800208392	0.024355121	0.546031898
0.001	**0.015087763**	**0.733360597**	**0.021306499**	**0.616375177**

0.01	0.041028619	0.273706974	0.043413704	0.234864208
0.1	0.056602334	4.27E-09	0.057069361	-0.029931029
1	0.056602334	4.27E-09	0.057069361	-0.029931029

ENR

hyper parameter		Regression result			
l1_ratio	alpha	MSE (training)	R^2 (training)	MSE (validation)	R^2 (validation)
0.3	0.001	0.011973131	0.788373443	0.022389517	0.58883475
0.3	0.005	0.015736512	0.721911266	0.022328867	0.600646611
0.3	0.01	0.019669904	0.652021549	0.024576333	0.567336219
0.3	0.05	0.041156261	0.27175795	0.04308714	0.243702218
0.3	0.1	0.053755648	0.049528148	0.05470799	0.022399118
0.3	0.5	0.056602334	0	0.057069362	-0.029931033
0.3	1	0.056602334	0	0.057069362	-0.029931033
0.5	0.001	0.012454493	0.77985791	0.021766916	0.601416456
0.5	0.005	0.017424541	0.692077694	0.023230615	0.587327171
0.5	0.01	0.022637358	0.599655275	0.025812876	0.552813834
0.5	0.05	0.04930378	0.128116178	0.05045746	0.10950693
0.5	0.1	0.056602334	0	0.057069362	-0.029931033
0.5	0.5	0.056602334	0	0.057069362	-0.029931033
0.5	1	0.056602334	0	0.057069362	-0.029931033
0.7	**0.001**	**0.012877068**	**0.772391626**	**0.021565477**	**0.605604885**
0.7	0.005	0.019073097	0.662960361	0.024091012	0.573401764
0.7	0.01	0.025423814	0.550243838	0.028590334	0.504191404
0.7	0.05	0.055361483	0.021309143	0.056150747	-0.00922199
0.7	0.1	0.056602334	0	0.057069362	-0.029931033
0.7	0.5	0.056602334	0	0.057069362	-0.029931033
0.7	1	0.056602334	0	0.057069362	-0.029931033

KRR

hyper parameter						Regression result			
kernel	alpha	degree	coef0	nu	length _scale	MSE (training)	R^2 (training)	MSE (validation)	R^2 (validation)
matern	0.001	x	x	0.5	1	1.26E-07	1	0.03131853	0.4479017
matern	0.001	x	x	0.5	10	7.16E-06	0.99987	0.02338267	0.6125445
matern	0.001	x	x	0.5	100	0.000353	0.99376	0.0231648	0.6139814

matern	0.001	x	x	1.5	1	1.16E-05	0.99979	0.030605	0.4562373
matern	0.001	x	x	1.5	10	0.002457	0.95656	0.02260727	0.5515607
matern	0.001	x	x	1.5	100	0.021522	0.6198	0.02712693	0.5208853
matern	0.001	x	x	2.5	1	2.79E-05	0.99951	0.03155413	0.4364936
matern	0.001	x	x	2.5	10	0.007219	0.87242	0.02340218	0.5601493
matern	0.001	x	x	2.5	100	0.026618	0.52978	0.03166495	0.4390331
matern	0.01	x	x	0.5	1	1.11E-05	0.9998	0.03145168	0.4448866
matern	0.01	x	x	0.5	10	3.65E-04	0.99356	0.02356186	0.6072166
matern	0.01	x	x	0.5	100	0.007061	0.87531	0.02582228	0.56127
matern	0.01	x	x	1.5	1	7.76E-05	0.99863	0.03033539	0.4608959
matern	0.01	x	x	1.5	10	0.0097	0.82848	0.02071587	0.5978812
matern	0.01	x	x	1.5	100	0.0447	0.20993	0.04772412	0.1502703
matern	0.01	x	x	2.5	1	0.000117	0.99793	0.03117043	0.4427243
matern	0.01	x	x	2.5	10	0.012983	0.77057	0.02179301	0.6088891
matern	0.01	x	x	2.5	100	0.048867	0.13642	0.0509655	0.0886685
matern	0.1	x	x	0.5	1	0.000677	0.98804	0.03276309	0.4171324
matern	0.1	x	x	0.5	10	0.007416	0.86903	0.02667446	0.5456935
matern	0.1	x	x	0.5	100	0.032241	0.43049	0.04078995	0.2752183
matern	0.1	x	x	1.5	1	0.001231	0.97824	0.03101435	0.4441463
matern	0.1	x	x	1.5	10	0.022742	0.59839	0.02911027	0.4844626
matern	0.1	x	x	1.5	100	0.054975	0.02876	0.05578959	-0.00583
matern	0.1	x	x	2.5	1	0.001623	0.97131	0.03138822	0.4343769
matern	0.1	x	x	2.5	10	0.026977	0.52344	0.03227501	0.4277512
matern	0.1	x	x	2.5	100	0.055657	0.01671	0.05632559	-0.015903
matern	1	x	x	0.5	1	0.01551	0.72582	0.04306339	0.2107791
matern	1	x	x	0.5	10	0.033683	0.405	0.04225081	0.2465299
matern	1	x	x	0.5	100	0.052385	0.07455	0.05429273	0.0227077
matern	1	x	x	1.5	1	0.016806	0.70289	0.03997971	0.2627323
matern	1	x	x	1.5	10	0.046585	0.17701	0.0492339	0.1160781
matern	1	x	x	1.5	100	0.056473	0.00228	0.05697739	-0.027873
matern	1	x	x	2.5	1	0.017643	0.68809	0.03965145	0.2633001
matern	1	x	x	2.5	10	0.049262	0.12971	0.0512775	0.0781172
matern	1	x	x	2.5	100	0.056546	0.001	0.05703365	-0.028926
linear	0.001	x	x	x	x	0.011142	0.80322	0.0265379	0.5046012
linear	0.01	x	x	x	x	0.011152	0.80305	0.02543495	0.5256411
linear	0.1	x	x	x	x	0.011554	0.79589	0.02232344	0.5864969
linear	1	x	x	x	x	0.014932	0.73615	0.02136055	0.6170885

poly	0.001	2	1	x	x	0.004166	0.92632	0.02650169	0.481971
poly	0.001	3	1	x	x	0.001863	0.9671	0.02842289	0.4005312
poly	0.001	4	1	x	x	0.000895	0.98421	0.03698163	0.314116
poly	0.01	2	1	x	x	0.009394	0.834	0.02236242	0.5844605
poly	0.01	3	1	x	x	0.00678	0.8801	0.02207427	0.5610954
poly	0.01	4	1	x	x	0.004681	0.91722	0.02312577	0.5384987
poly	0.1	2	1	x	x	0.015438	0.72723	0.02235553	0.6025348
poly	0.1	3	1	x	x	0.012904	0.77198	0.02182598	0.6082886
poly	0.1	4	1	x	x	0.011049	0.80465	0.02039386	0.6057275
poly	1	2	1	x	x	0.034368	0.39285	0.0387839	0.3077806
poly	1	3	1	x	x	0.027896	0.50719	0.03319374	0.4095484
poly	1	4	1	x	x	0.023232	0.58959	0.02922984	0.4811393
rbf	0.001	x	x	x	x	0.002876	0.9492	0.02551404	0.4699683
rbf	0.01	x	x	x	x	0.008537	0.84903	0.02109657	0.5819734
rbf	0.1	x	x	x	x	0.016385	0.7105	0.02386318	0.5752583
rbf	1	x	x	x	x	0.03725	0.34192	0.04150431	0.2570324
sigmoid	0.001	x	1	x	x	0.074878	-0.32517	0.05748358	-0.133501
sigmoid	**0.01**	**x**	**1**	**x**	**x**	**0.01614**	**0.7147**	**0.021063**	**0.624649**
sigmoid	0.1	x	1	x	x	0.031364	0.44593	0.03569768	0.3650124
sigmoid	1	x	1	x	x	0.051315	0.09345	0.05282752	0.0496871

BRR

hyper parameter	Regression result			
tol	MSE (training)	R^2 (training)	MSE (validation)	R^2 (validation)
0.00001	**0.013037243**	**0.769688218**	**0.021596336**	**0.606056148**
0.0001	0.013037233	0.769688396	0.021596336	0.60605609
0.001	0.013037151	0.769689843	0.021596338	0.606055674
0.01	0.013036234	0.769706092	0.021596291	0.606053311
0.1	0.013025769	0.76989143	0.021595167	0.606046599

ARD

hyper parameter				Regression result			
alpha_1	alpha_2	lambda_1	lambda_2	MSE (training)	R^2 (training)	MSE (validation)	R^2 (validation)
1.00E-04	1.00E-04	1.00E-04	1.00E-04	0.0136	0.7592	0.0217	0.6034
1.00E-04	1.00E-04	1.00E-04	1.00E-06	0.0140	0.7520	0.0213	0.6118

1.00E-04	1.00E-04	1.00E-04	1.00E-08	0.0140	0.7532	0.0210	0.6092
1.00E-04	1.00E-04	1.00E-06	1.00E-04	0.0136	0.7592	0.0217	0.6034
1.00E-04	1.00E-04	1.00E-06	1.00E-06	0.0140	0.7520	0.0213	0.6118
1.00E-04	1.00E-04	1.00E-06	1.00E-08	0.0140	0.7532	0.0210	0.6092
1.00E-04	1.00E-04	1.00E-08	1.00E-04	0.0136	0.7592	0.0217	0.6034
1.00E-04	1.00E-04	1.00E-08	1.00E-06	0.0140	0.7520	0.0213	0.6118
1.00E-04	1.00E-04	1.00E-08	1.00E-08	0.0140	0.7532	0.0210	0.6092
1.00E-04	1.00E-06	1.00E-04	1.00E-04	0.0136	0.7592	0.0217	0.6034
1.00E-04	1.00E-06	1.00E-04	1.00E-06	0.0140	0.7520	0.0213	0.6118
1.00E-04	1.00E-06	1.00E-04	1.00E-08	0.0140	0.7532	0.0210	0.6092
1.00E-04	1.00E-06	1.00E-06	1.00E-04	0.0136	0.7593	0.0217	0.6034
1.00E-04	1.00E-06	1.00E-06	1.00E-06	0.0140	0.7520	0.0213	0.6118
1.00E-04	1.00E-06	1.00E-06	1.00E-08	0.0140	0.7532	0.0210	0.6092
1.00E-04	1.00E-06	1.00E-08	1.00E-04	0.0136	0.7593	0.0217	0.6034
1.00E-04	1.00E-06	1.00E-08	1.00E-06	0.0140	0.7520	0.0213	0.6118
1.00E-04	1.00E-06	1.00E-08	1.00E-08	0.0140	0.7532	0.0210	0.6092
1.00E-04	1.00E-08	1.00E-04	1.00E-04	0.0136	0.7592	0.0217	0.6034
1.00E-04	1.00E-08	1.00E-04	1.00E-06	0.0140	0.7520	0.0213	0.6118
1.00E-04	1.00E-08	1.00E-04	1.00E-08	0.0140	0.7532	0.0210	0.6092
1.00E-04	1.00E-08	1.00E-06	1.00E-04	0.0136	0.7593	0.0217	0.6034
1.00E-04	1.00E-08	1.00E-06	1.00E-06	0.0140	0.7520	0.0213	0.6118
1.00E-04	1.00E-08	1.00E-06	1.00E-08	0.0140	0.7532	0.0210	0.6092
1.00E-04	1.00E-08	1.00E-08	1.00E-04	0.0136	0.7593	0.0217	0.6034
1.00E-04	1.00E-08	1.00E-08	1.00E-06	0.0140	0.7520	0.0213	0.6118
1.00E-04	1.00E-08	1.00E-08	1.00E-08	0.0140	0.7532	0.0210	0.6092
1.00E-06	1.00E-04	1.00E-04	1.00E-04	0.0136	0.7592	0.0217	0.6034
1.00E-06	1.00E-04	1.00E-04	1.00E-06	0.0140	0.7520	0.0213	0.6118
1.00E-06	1.00E-04	1.00E-04	1.00E-08	0.0140	0.7532	0.0210	0.6092
1.00E-06	1.00E-04	1.00E-06	1.00E-04	0.0136	0.7592	0.0217	0.6034
1.00E-06	1.00E-04	1.00E-06	1.00E-06	0.0140	0.7520	0.0213	0.6118
1.00E-06	1.00E-04	1.00E-06	1.00E-08	0.0140	0.7532	0.0210	0.6092
1.00E-06	1.00E-04	1.00E-08	1.00E-04	0.0136	0.7592	0.0217	0.6034
1.00E-06	1.00E-04	1.00E-08	1.00E-06	0.0140	0.7520	0.0213	0.6118
1.00E-06	1.00E-04	1.00E-08	1.00E-08	0.0140	0.7532	0.0210	0.6092
1.00E-06	1.00E-06	1.00E-04	1.00E-04	0.0136	0.7592	0.0217	0.6034
1.00E-06	1.00E-06	1.00E-04	1.00E-06	0.0140	0.7520	0.0213	0.6118
1.00E-06	1.00E-06	1.00E-04	1.00E-08	0.0140	0.7532	0.0210	0.6092

1.00E-06	1.00E-06	1.00E-06	1.00E-04	0.0136	0.7593	0.0217	0.6034
1.00E-06	1.00E-06	1.00E-06	1.00E-06	0.0140	0.7520	0.0213	0.6118
1.00E-06	1.00E-06	1.00E-06	1.00E-08	0.0140	0.7532	0.0210	0.6092
1.00E-06	1.00E-06	1.00E-08	1.00E-04	0.0136	0.7593	0.0217	0.6034
1.00E-06	1.00E-06	1.00E-08	1.00E-06	0.0140	0.7520	0.0213	0.6118
1.00E-06	1.00E-06	1.00E-08	1.00E-08	0.0140	0.7532	0.0210	0.6092
1.00E-06	1.00E-08	1.00E-04	1.00E-04	0.0136	0.7592	0.0217	0.6034
1.00E-06	1.00E-08	1.00E-04	1.00E-06	0.0140	0.7520	0.0213	0.6118
1.00E-06	1.00E-08	1.00E-04	1.00E-08	0.0140	0.7532	0.0210	0.6092
1.00E-06	1.00E-08	1.00E-06	1.00E-04	0.0136	0.7593	0.0217	0.6034
1.00E-06	1.00E-08	1.00E-06	1.00E-06	0.0140	0.7520	0.0213	0.6118
1.00E-06	1.00E-08	1.00E-06	1.00E-08	0.0140	0.7532	0.0210	0.6092
1.00E-06	1.00E-08	1.00E-08	1.00E-04	0.0136	0.7593	0.0217	0.6034
1.00E-06	1.00E-08	1.00E-08	1.00E-06	0.0140	0.7520	0.0213	0.6118
1.00E-06	1.00E-08	1.00E-08	1.00E-08	0.0140	0.7532	0.0210	0.6092
1.00E-08	1.00E-04	1.00E-04	1.00E-04	0.0136	0.7592	0.0217	0.6034
1.00E-08	**1.00E-04**	**1.00E-04**	**1.00E-06**	**0.0140**	**0.7520**	**0.0213**	**0.6118**
1.00E-08	1.00E-04	1.00E-04	1.00E-08	0.0140	0.7532	0.0210	0.6092
1.00E-08	1.00E-04	1.00E-06	1.00E-04	0.0136	0.7592	0.0217	0.6034
1.00E-08	1.00E-04	1.00E-06	1.00E-06	0.0140	0.7520	0.0213	0.6118
1.00E-08	1.00E-04	1.00E-06	1.00E-08	0.0140	0.7532	0.0210	0.6092
1.00E-08	1.00E-04	1.00E-08	1.00E-04	0.0136	0.7592	0.0217	0.6034
1.00E-08	1.00E-04	1.00E-08	1.00E-06	0.0140	0.7520	0.0213	0.6118
1.00E-08	1.00E-04	1.00E-08	1.00E-08	0.0140	0.7532	0.0210	0.6092
1.00E-08	1.00E-06	1.00E-04	1.00E-04	0.0136	0.7592	0.0217	0.6034
1.00E-08	1.00E-06	1.00E-04	1.00E-06	0.0140	0.7520	0.0213	0.6118
1.00E-08	1.00E-06	1.00E-04	1.00E-08	0.0140	0.7532	0.0210	0.6092
1.00E-08	1.00E-06	1.00E-06	1.00E-04	0.0136	0.7593	0.0217	0.6034
1.00E-08	1.00E-06	1.00E-06	1.00E-06	0.0140	0.7520	0.0213	0.6118
1.00E-08	1.00E-06	1.00E-06	1.00E-08	0.0140	0.7532	0.0210	0.6092
1.00E-08	1.00E-06	1.00E-08	1.00E-04	0.0136	0.7593	0.0217	0.6034
1.00E-08	1.00E-06	1.00E-08	1.00E-06	0.0140	0.7520	0.0213	0.6118
1.00E-08	1.00E-06	1.00E-08	1.00E-08	0.0140	0.7532	0.0210	0.6092
1.00E-08	1.00E-08	1.00E-04	1.00E-04	0.0136	0.7592	0.0217	0.6034
1.00E-08	1.00E-08	1.00E-04	1.00E-06	0.0140	0.7520	0.0213	0.6118
1.00E-08	1.00E-08	1.00E-04	1.00E-08	0.0410	0.2737	0.0434	0.2349
1.00E-08	1.00E-08	1.00E-06	1.00E-04	0.0136	0.7593	0.0217	0.6034

1.00E-08	1.00E-08	1.00E-06	1.00E-06	0.0140	0.7520	0.0213	0.6118
1.00E-08	1.00E-08	1.00E-06	1.00E-08	0.0140	0.7532	0.0210	0.6092
1.00E-08	1.00E-08	1.00E-08	1.00E-04	0.0136	0.7593	0.0217	0.6034
1.00E-08	1.00E-08	1.00E-08	1.00E-06	0.0140	0.7520	0.0213	0.6118
1.00E-08	1.00E-08	1.00E-08	1.00E-08	0.0140	0.7532	0.0210	0.6092

RF

hyper parameter			Regression result			
max_features	n_estimators	max_depth	MSE (training)	R^2 (training)	MSE (validation)	R^2 (validation)
auto	50	5	0.006265	0.889339	0.02501878	0.54913132
auto	50	10	0.00351	0.938009	0.02381634	0.56988986
auto	50	15	0.003493	0.938304	0.02409065	0.56634305
auto	100	5	0.005802	0.897588	0.02498501	0.54967559
auto	100	10	0.003692	0.934824	0.02353246	0.56650378
auto	100	15	0.003672	0.935192	0.02375659	0.56827481
auto	150	5	0.005819	0.897301	0.02498908	0.54782883
auto	150	10	0.00357	0.937025	0.02361944	0.5693722
auto	150	15	0.003542	0.937531	0.0237654	0.57142196
log2	50	5	0.00875	0.845578	0.02760483	0.53312746
log2	50	10	0.003867	0.931674	0.02494953	0.56857106
log2	50	15	0.003708	0.934487	0.0250613	0.55381279
log2	100	5	0.008263	0.853761	0.025563	0.53026635
log2	100	10	0.003805	0.932805	0.02440948	0.58343255
log2	100	15	0.00369	0.934843	0.02442876	0.57774216
log2	150	5	0.008465	0.850591	0.02659496	0.5359652
log2	150	10	0.003719	0.934377	0.02485223	0.57801827
log2	150	15	0.003593	0.936573	0.02480667	0.57089401
sqrt	50	5	0.008107	0.857104	0.0256093	0.55939493
sqrt	50	10	0.003587	0.936607	0.02388609	0.58032151
sqrt	50	15	0.003419	0.939549	0.02402252	0.57666628
sqrt	100	5	0.007639	0.865291	0.02546824	0.56099945
sqrt	**100**	**10**	**0.00381**	**0.93277**	**0.024784**	**0.584808**
sqrt	100	15	0.003731	0.934136	0.02492709	0.58205772
sqrt	150	5	0.007801	0.862382	0.02568271	0.55288677
sqrt	150	10	0.003697	0.934693	0.02494066	0.58350872
sqrt	150	15	0.003592	0.936602	0.02459363	0.57459597

Ada Boost

hyper parameter			Regression result			
loss	learning_rate	n_estimators	MSE (training)	R^2 (training)	MSE (validation)	R^2 (validation)
exponential	0.001	50	0.0128073	0.7734752	0.0235366	0.5528765
exponential	0.001	100	0.012578	0.7774871	0.0236956	0.5517866
exponential	0.001	150	0.0125845	0.7774758	0.023575	0.5523912
exponential	0.01	50	0.0125959	0.7771389	0.023451	0.5444425
exponential	0.01	100	0.0116067	0.7947896	0.0238186	0.5478957
exponential	0.01	150	0.0112957	0.8002147	0.0243393	0.5414988
exponential	0.1	50	0.0097695	0.8268483	0.0253087	0.5333856
exponential	0.1	100	0.0074695	0.8680207	0.0265683	0.5284115
exponential	0.1	150	0.0068324	0.8792013	0.0269827	0.5199567
exponential	1	50	0.0059872	0.8945366	0.0279726	0.5209833
exponential	1	100	0.0054484	0.9039119	0.0279125	0.5181311
exponential	1	150	0.0052733	0.9069571	0.0281329	0.5167544
linear	0.001	50	0.0127434	0.7745927	0.024029	0.5474231
linear	0.001	100	0.0125119	0.7786686	0.0235107	0.5540541
linear	0.001	150	0.0124667	0.7795665	0.0235431	0.5521346
linear	0.01	50	0.0121262	0.7854384	0.0239915	0.55049
linear	0.01	100	0.0114782	0.7969406	0.0244402	0.5375357
linear	0.01	150	0.0111108	0.8034352	0.0241377	0.5437199
linear	0.1	50	0.0088564	0.8435887	0.0264506	0.5283151
linear	0.1	100	0.0071266	0.8739756	0.0272125	0.5245813
linear	0.1	150	0.006376	0.8871389	0.0280891	0.503078
linear	1	50	0.0058718	0.8962546	0.0280578	0.491944
linear	1	100	0.0053679	0.9051528	0.0281221	0.4916817
linear	1	150	0.0052153	0.9078432	0.0274242	0.5078048
square	0.001	50	0.0127342	0.7746455	0.0237136	0.5443726
square	0.001	100	0.0123474	0.7815	0.0235682	0.5542917
square	0.001	150	0.01221	0.7839894	0.0232305	0.5572812
square	**0.01**	**50**	**0.012077**	**0.786293**	**0.023448**	**0.557679**
square	0.01	100	0.0112185	0.8019832	0.0249577	0.5454058
square	0.01	150	0.0104369	0.8153431	0.0250689	0.534722
square	0.1	50	0.0075749	0.8661449	0.02627	0.52551
square	0.1	100	0.0063166	0.8883163	0.0287999	0.5182371

square	0.1	150	0.0056404	0.9001498	0.0295952	0.5082768
square	1	50	0.005683	0.8988169	0.0270855	0.5151965
square	1	100	0.0051616	0.9086575	0.0277572	0.506882
square	1	150	0.0050632	0.9100322	0.026487	0.5076237

Gradient Boost

hyper parameter				Regression result			
loss	learning _rate	n_estimators	sub sample	MSE (training)	R^2 (training)	MSE (validation)	R^2 (validation)
huber	0.001	50	0.4	0.053311	0.058174	0.054439	0.017310
huber	0.001	50	0.7	0.052883	0.065717	0.054256	0.020409
huber	0.001	50	1	0.052697	0.069013	0.054410	0.017722
huber	0.001	100	0.4	0.050190	0.113294	0.052000	0.062458
huber	0.001	100	0.7	0.049398	0.127295	0.051707	0.066920
huber	0.001	100	1	0.049027	0.133727	0.051704	0.064291
huber	0.001	150	0.4	0.047342	0.163626	0.049746	0.103369
huber	0.001	150	0.7	0.046191	0.183956	0.049261	0.111805
huber	0.001	150	1	0.045719	0.192157	0.049404	0.105973
huber	0.01	50	0.4	0.032212	0.430971	0.038337	0.314208
huber	0.01	50	0.7	0.029849	0.472670	0.037556	0.324575
huber	0.01	50	1	0.029291	0.482231	0.037934	0.315188
huber	0.01	100	0.4	0.020358	0.640373	0.030726	0.454647
huber	0.01	100	0.7	0.017945	0.683205	0.031089	0.456210
huber	0.01	100	1	0.017754	0.685998	0.030708	0.450484
huber	0.01	150	0.4	0.014248	0.748308	0.027215	0.518115
huber	0.01	150	0.7	0.012072	0.786868	0.028193	0.509172
huber	0.01	150	1	0.011902	0.789493	0.028043	0.490404
huber	0.1	50	0.4	0.003977	0.929837	0.023603	0.575101
huber	0.1	50	0.7	0.002244	0.960401	0.022259	0.557828
huber	0.1	50	1	0.002406	0.957715	0.025781	0.500116
huber	0.1	100	0.4	0.001106	0.980534	0.025100	0.541436
huber	0.1	100	0.7	0.000535	0.990576	0.024932	0.532744
huber	0.1	100	1	0.000711	0.987397	0.026240	0.512479
huber	0.1	150	0.4	0.000321	0.994340	0.025672	0.519463
huber	0.1	150	0.7	0.000204	0.996397	0.025087	0.531197
huber	0.1	150	1	0.000296	0.994722	0.025935	0.516588

huber	1	50	0.4	0.040513	0.248420	0.387526	-7.198172
huber	1	50	0.7	0.000031	0.999455	0.044250	0.076384
huber	1	50	1	0.000028	0.999507	0.033296	0.318763
huber	1	100	0.4	0.019056	0.657426	0.650754	-13.809753
huber	1	100	0.7	0.000007	0.999877	0.044542	0.065520
huber	1	100	1	0.000008	0.999845	0.033602	0.312272
huber	1	150	0.4	0.029667	0.473757	1.906096	-34.783053
huber	1	150	0.7	0.000001	0.999989	0.044537	0.065616
huber	1	150	1	0.000000	1.000000	0.033602	0.312272
lad	0.001	50	0.4	0.054446	0.038111	0.055445	-0.000020
lad	0.001	50	0.7	0.054161	0.043136	0.055288	0.002448
lad	0.001	50	1	0.054053	0.044993	0.055202	0.003914
lad	0.001	100	0.4	0.052316	0.075760	0.053800	0.030902
lad	0.001	100	0.7	0.051705	0.086506	0.053529	0.035627
lad	0.001	100	1	0.051473	0.090507	0.053425	0.037148
lad	0.001	150	0.4	0.050416	0.109340	0.052393	0.057752
lad	0.001	150	0.7	0.049408	0.127097	0.051828	0.067637
lad	0.001	150	1	0.048885	0.135883	0.051613	0.070571
lad	0.01	50	0.4	0.038820	0.314336	0.043932	0.217919
lad	0.01	50	0.7	0.037073	0.344928	0.042985	0.245587
lad	0.01	50	1	0.036161	0.360654	0.040753	0.262433
lad	0.01	100	0.4	0.029283	0.482521	0.037421	0.349591
lad	0.01	100	0.7	0.026977	0.523336	0.036009	0.373888
lad	0.01	100	1	0.025627	0.546635	0.033565	0.382197
lad	0.01	150	0.4	0.023788	0.579652	0.034230	0.408375
lad	0.01	150	0.7	0.021119	0.626905	0.032366	0.431193
lad	0.01	150	1	0.019945	0.647193	0.030345	0.434531
lad	0.1	50	0.4	0.010361	0.816666	0.026610	0.537512
lad	0.1	50	0.7	0.008650	0.847269	0.023951	0.579504
lad	0.1	50	1	0.009760	0.827484	0.026450	0.533093
lad	0.1	100	0.4	0.005623	0.900291	0.024893	0.550601
lad	**0.1**	**100**	**0.7**	**0.004666**	**0.917573**	**0.023405**	**0.589600**
lad	0.1	100	1	0.006582	0.883732	0.024524	0.563759
lad	0.1	150	0.4	0.003798	0.932661	0.024378	0.558372
lad	0.1	150	0.7	0.003456	0.938948	0.023504	0.587246
lad	0.1	150	1	0.005226	0.907716	0.024076	0.570612
lad	1	50	0.4	0.037828	0.334296	0.170443	-2.491508

lad	1	50	0.7	0.001394	0.975414	0.044836	0.150390
lad	1	50	1	0.001564	0.972339	0.035230	0.258057
lad	1	100	0.4	0.019001	0.642944	0.320614	-5.103614
lad	1	100	0.7	0.000891	0.984194	0.045288	0.145838
lad	1	100	1	0.000949	0.983450	0.033705	0.283919
lad	1	150	0.4	0.019965	0.625431	0.416251	-6.174923
lad	1	150	0.7	0.000283	0.995037	0.046234	0.122259
lad	1	150	1	0.000853	0.985094	0.033707	0.283898
ls	0.001	50	0.4	0.053219	0.059779	0.054381	0.019616
ls	0.001	50	0.7	0.052776	0.067609	0.054231	0.021911
ls	0.001	50	1	0.052595	0.070728	0.053949	0.020700
ls	0.001	100	0.4	0.050124	0.114461	0.051961	0.064393
ls	0.001	100	0.7	0.049302	0.128995	0.051709	0.067970
ls	0.001	100	1	0.048961	0.134932	0.051386	0.066358
ls	0.001	150	0.4	0.047310	0.164199	0.049755	0.104464
ls	0.001	150	0.7	0.046102	0.185519	0.049303	0.112108
ls	0.001	150	1	0.045656	0.193308	0.049116	0.105945
ls	0.01	50	0.4	0.032162	0.431806	0.038664	0.310690
ls	0.01	50	0.7	0.029852	0.472572	0.037255	0.316411
ls	0.01	50	1	0.028921	0.489157	0.038800	0.326153
ls	0.01	100	0.4	0.021013	0.628732	0.032046	0.449656
ls	0.01	100	0.7	0.017621	0.688853	0.031030	0.459427
ls	0.01	100	1	0.016418	0.709695	0.031048	0.448221
ls	0.01	150	0.4	0.014606	0.741955	0.028961	0.508164
ls	0.01	150	0.7	0.011481	0.797293	0.028139	0.506978
ls	0.01	150	1	0.010334	0.817259	0.028044	0.484298
ls	0.1	50	0.4	0.003225	0.943040	0.027453	0.535444
ls	0.1	50	0.7	0.001768	0.968749	0.025197	0.550150
ls	0.1	50	1	0.001475	0.973994	0.025486	0.525167
ls	0.1	100	0.4	0.000809	0.985724	0.027704	0.527158
ls	0.1	100	0.7	0.000260	0.995419	0.024103	0.550833
ls	0.1	100	1	0.000250	0.995592	0.025167	0.528867
ls	0.1	150	0.4	0.000252	0.995541	0.028083	0.523693
ls	0.1	150	0.7	0.000051	0.999108	0.024436	0.544882
ls	0.1	150	1	0.000051	0.999105	0.025443	0.522908
ls	1	50	0.4	0.005735	0.897930	0.192536	-2.871815
ls	1	50	0.7	0.000000	0.999997	0.044318	0.219472

ls	1	50	1	0.000000	1.000000	0.038446	0.262652
ls	1	100	0.4	0.000772	0.986583	0.215188	-3.311827
ls	1	100	0.7	0.000000	1.000000	0.044305	0.219639
ls	1	100	1	0.000000	1.000000	0.038446	0.262651
ls	1	150	0.4	0.000255	0.995669	0.226206	-3.588967
ls	1	150	0.7	0.000000	1.000000	0.044305	0.219639
ls	1	150	1	0.000000	1.000000	0.038446	0.262651
quantile	0.001	50	0.4	0.151229	-1.671774	0.151878	-1.795931
quantile	0.001	50	0.7	0.151154	-1.670483	0.151938	-1.796998
quantile	0.001	50	1	0.150867	-1.665381	0.151996	-1.798529
quantile	0.001	100	0.4	0.147007	-1.597240	0.148013	-1.722924
quantile	0.001	100	0.7	0.147046	-1.597913	0.148267	-1.727915
quantile	0.001	100	1	0.146393	-1.586320	0.148269	-1.728638
quantile	0.001	150	0.4	0.142911	-1.524915	0.144205	-1.651048
quantile	0.001	150	0.7	0.143190	-1.529814	0.144880	-1.664004
quantile	0.001	150	1	0.142246	-1.513059	0.144762	-1.662716
quantile	0.01	50	0.4	0.121599	-1.148346	0.124337	-1.275341
quantile	0.01	50	0.7	0.121590	-1.148286	0.125460	-1.298555
quantile	0.01	50	1	0.119527	-1.111724	0.125743	-1.305094
quantile	0.01	100	0.4	0.100653	-0.778400	0.105631	-0.926883
quantile	0.01	100	0.7	0.101293	-0.789700	0.107981	-0.970288
quantile	0.01	100	1	0.099231	-0.752944	0.108667	-0.985331
quantile	0.01	150	0.4	0.085740	-0.514921	0.092269	-0.678438
quantile	0.01	150	0.7	0.087217	-0.541710	0.095571	-0.755262
quantile	0.01	150	1	0.086643	-0.530655	0.098580	-0.793263
quantile	0.1	50	0.4	0.048395	0.143895	0.060823	-0.095065
quantile	0.1	50	0.7	0.055950	0.009540	0.071365	-0.328745
quantile	0.1	50	1	0.061365	-0.085617	0.073400	-0.428200
quantile	0.1	100	0.4	0.034664	0.386122	0.046103	0.121433
quantile	0.1	100	0.7	0.043651	0.228280	0.061017	-0.136535
quantile	0.1	100	1	0.056294	0.002713	0.067978	-0.316414
quantile	0.1	150	0.4	0.023783	0.579283	0.038511	0.228323
quantile	0.1	150	0.7	0.038068	0.326463	0.056744	-0.040353
quantile	0.1	150	1	0.054010	0.042992	0.066355	-0.289750
quantile	1	50	0.4	0.054811	0.032305	0.077344	-0.696832
quantile	1	50	0.7	0.027925	0.504773	0.058226	-0.199228
quantile	1	50	1	0.031446	0.441604	0.062035	-0.227860

quantile	1	100	0.4	0.057434	-0.031394	0.085030	-0.894807
quantile	1	100	0.7	0.015643	0.721964	0.062309	-0.527011
quantile	1	100	1	0.021433	0.618733	0.066064	-0.277720
quantile	1	150	0.4	0.060431	-0.068258	0.093435	-0.807615
quantile	1	150	0.7	0.012271	0.783897	0.074433	-0.654087
quantile	1	150	1	0.018333	0.674424	0.066838	-0.266111

XG Boost

hyper parameter			Regression result			
learning_rate	sub sample	max_depth	MSE (training)	R^2 (training)	MSE (validation)	R^2 (validation)
0.001	0.4	4	0.05147215	0.090660167	5.28E-02	0.04957626
0.001	0.4	6	0.05138633	0.092172567	5.28E-02	0.04987045
0.001	0.4	8	0.05138557	0.092188211	5.28E-02	0.04994082
0.001	0.7	4	0.05000295	0.116604585	5.22E-02	0.06041824
0.001	0.7	6	0.04965833	0.122693	5.22E-02	0.06061206
0.001	0.7	8	0.04960454	0.123641752	5.22E-02	0.06073516
0.001	1	4	0.04933414	0.128241282	5.18E-02	0.05742117
0.001	1	6	0.04866122	0.140159184	5.16E-02	0.05973683
0.001	1	8	0.04850253	0.142961426	5.15E-02	0.06064209
0.01	0.4	4	0.02418521	0.572746794	3.40E-02	0.39816787
0.01	0.4	6	0.02366603	0.58193711	3.37E-02	0.40325634
0.01	0.4	8	0.0236438	0.582320553	3.36E-02	0.40425332
0.01	0.7	4	0.01819029	0.678263398	3.13E-02	0.42528324
0.01	0.7	6	0.01632819	0.711258396	3.11E-02	0.42980245
0.01	0.7	8	0.01601635	0.716784201	0.031198937	0.42767226
0.01	1	4	0.01556133	0.724668301	0.03276885	0.40636608
0.01	1	6	0.01281377	0.773446077	0.034293786	0.40917066
0.01	1	8	0.01226617	0.783230033	0.035385954	0.39513923
0.1	**0.4**	**4**	**0.0009681**	**0.9828959**	**0.0265561**	**0.5288735**
0.1	0.4	6	0.00082428	0.985384681	0.02661654	0.52584901
0.1	0.4	8	0.00069344	0.987747978	0.027590032	0.50373683
0.1	0.7	4	0.00013889	0.997541748	0.027516305	0.49826606
0.1	0.7	6	2.08E-05	0.999631675	0.027406935	0.48284666
0.1	0.7	8	1.10E-05	0.999806257	0.026204192	0.50147677
0.1	1	4	8.43E-05	0.998517036	0.031750354	0.456443
0.1	1	6	1.68E-06	0.999969938	0.029610079	0.41672305

0.1	1	8	5.49E-07	0.999990216	0.030357139	0.39421961
1	0.4	4	4.01E-06	0.999928988	0.062869034	-0.2468915
1	0.4	6	1.10E-06	0.999980459	0.054771074	-0.1998166
1	0.4	8	1.25E-06	0.999977994	0.043820433	-0.0381041
1	0.7	4	1.14E-07	0.999997963	0.03121231	0.31103509
1	0.7	6	1.04E-07	0.999998148	0.028896427	0.37041169
1	0.7	8	1.04E-07	0.999998164	0.037201529	0.26491071
1	1	4	2.53E-07	0.999995557	0.029842835	0.40073018
1	1	6	2.12E-07	0.999996247	0.033354248	0.33005985
1	1	8	1.79E-07	0.999996817	0.031678236	0.35431096

SVR

hyper parameter					Regression result			
kernel	C	degree	nu	length _scale	MSE (training)	R^2 (training)	MSE (validation)	R^2 (validation)
matern	0.001	x	0.5	1	0.0563258	0.004648	0.05698656	-0.0333315
matern	0.001	x	0.5	10	0.0567224	-0.002367	0.05717137	-0.0368998
matern	0.001	x	0.5	100	0.0568435	-0.004508	0.05724033	-0.0381642
matern	0.001	x	1.5	1	0.0562376	0.006205	0.05689147	-0.0316411
matern	0.001	x	1.5	10	0.0568154	-0.004011	0.05722218	-0.0378316
matern	0.001	x	1.5	100	0.0568581	-0.004767	0.05724873	-0.0383183
matern	0.001	x	2.5	1	0.056209	0.006709	0.05686163	-0.031128
matern	0.001	x	2.5	10	0.0568293	-0.004257	0.05723084	-0.0379896
matern	0.001	x	2.5	100	0.0568584	-0.004771	0.05724888	-0.0383209
matern	0.01	x	0.5	1	0.0519637	0.081806	0.05479188	0.0097059
matern	0.01	x	0.5	10	0.0555133	0.019007	0.05646303	-0.0235447
matern	0.01	x	0.5	100	0.056707	-0.002096	0.05716189	-0.0367257
matern	0.01	x	1.5	1	0.0512979	0.093824	0.05403078	0.027884
matern	0.01	x	1.5	10	0.0564276	0.00284	0.05697638	-0.0332981
matern	0.01	x	1.5	100	0.0568533	-0.004681	0.05724573	-0.038263
matern	0.01	x	2.5	1	0.0510771	0.097734	0.05373051	0.03349901
matern	0.01	x	2.5	10	0.0565653	0.000406	0.05706543	-0.0349575
matern	0.01	x	2.5	100	0.0568556	-0.004722	0.05724717	-0.0382894
matern	0.1	x	0.5	1	0.0267197	0.528186	0.04171525	0.2584265
matern	0.1	x	0.5	10	0.0457843	0.191304	0.04996154	0.10294563
matern	0.1	x	0.5	100	0.0553649	0.02163	0.05636011	-0.0214527
matern	0.1	x	1.5	1	0.0257019	0.546126	0.03799745	0.32616166

matern	0.1	x	1.5	10	0.0528141	0.066697	0.05429453	0.01996075
matern	0.1	x	1.5	100	0.0568046	-0.003821	0.05721569	-0.0377107
matern	0.1	x	2.5	1	0.0256927	0.54625	0.03719137	0.3406822
matern	0.1	x	2.5	10	0.0540495	0.044863	0.05522418	0.00136402
matern	0.1	x	2.5	100	0.0568279	-0.004232	0.05723007	-0.037975
matern	1	x	0.5	1	0.0068105	0.879344	0.03145867	0.42762708
matern	1	x	0.5	10	0.015221	0.731252	0.03079637	0.47107006
matern	1	x	0.5	100	0.0448185	0.208383	0.04912426	0.11827902
matern	1	x	1.5	1	0.0066627	0.881965	0.02792119	0.49599562
matern	1	x	1.5	10	0.0340022	0.399421	0.03824465	0.31972809
matern	1	x	1.5	100	0.0563212	0.004721	0.0569092	-0.0320442
matern	1	x	2.5	1	0.0065785	0.883472	0.02748523	0.50402411
matern	1	x	2.5	10	0.0389892	0.3113	0.0419866	0.24979956
matern	1	x	2.5	100	0.0565518	0.000645	0.05705738	-0.0348051
linear	0.001	x	x	x	0.0550559	0.027083	0.05600101	-0.014311
linear	0.01	x	x	x	0.0433934	0.233021	0.04603792	0.1764199
linear	0.1	x	x	x	0.019265	0.659625	0.02503753	0.5578633
linear	**1**	**x**	**x**	**x**	**0.013179**	**0.76722**	**0.0200605**	**0.6297952**
poly	0.001	2	x	x	0.0371927	0.343042	0.04110684	0.26587554
poly	0.001	3	x	x	0.0313702	0.445946	0.03646319	0.35170277
poly	0.001	4	x	x	0.0272819	0.518071	0.03297553	0.41748968
poly	0.01	2	x	x	0.0149733	0.73561	0.02429391	0.56729902
poly	0.01	3	x	x	0.0134429	0.762363	0.02170956	0.58155115
poly	0.01	4	x	x	0.0124474	0.779996	0.02260336	0.58829283
poly	0.1	2	x	x	0.0081319	0.856208	0.02370681	0.53402042
poly	0.1	3	x	x	0.0077095	0.863627	0.02530719	0.49770565
poly	0.1	4	x	x	0.0073691	0.869591	0.02615543	0.48021836
poly	1	2	x	x	0.0069863	0.876256	0.02615785	0.48913085
poly	1	3	x	x	0.0069871	0.876234	0.02664776	0.47411996
poly	1	4	x	x	0.0070019	0.875971	0.02720345	0.45859991
rbf	0.001	x	x	x	0.0562069	0.006744	0.05683144	-0.0306358
rbf	0.01	x	x	x	0.0510642	0.097963	0.05334833	0.04015558
rbf	0.1	x	x	x	0.0274863	0.514472	0.03590628	0.36360126
rbf	1	x	x	x	0.0089311	0.842244	0.02828517	0.53111811
sigmoid	0.001	x	x	x	0.0568022	-0.003779	0.05720824	-0.037544
sigmoid	0.01	x	x	x	0.0562973	0.005133	0.05683757	-0.0305709
sigmoid	0.1	x	x	x	0.0520108	0.081212	0.05340705	0.03788294

sigmoid	1	x	x	x	0.0353527	0.375336	0.03583478	0.35406766

KNN

hyper parameter			Regression result			
weights	n_neighbors	p	MSE (training)	R^2 (training)	MSE (validation)	R^2 (validation)
distance	**3**	**1**	**0**	**1**	**0.026756**	**0.4846771**
distance	3	2	0	1	0.03257736	0.38918737
distance	5	1	0	1	0.03054621	0.42041944
distance	5	2	0	1	0.0350297	0.3539005
distance	7	1	0	1	0.03185241	0.39410981
distance	7	2	0	1	0.03588907	0.33130834
distance	11	1	0	1	0.03203239	0.39135899
distance	11	2	0	1	0.03833145	0.3241954
distance	13	1	0	1	0.03309077	0.3681066
distance	13	2	0	1	0.04029236	0.28508985
uniform	3	1	0.018204	0.678183	0.03301956	0.39843033
uniform	3	2	0.021632	0.617805	0.03479548	0.34358904
uniform	5	1	0.025729	0.545474	0.03827157	0.31525843
uniform	5	2	0.026497	0.532133	0.04076233	0.27938469
uniform	7	1	0.030515	0.461096	0.03747982	0.27246362
uniform	7	2	0.032854	0.41948	0.03949741	0.25928803
uniform	11	1	0.034607	0.388084	0.03590689	0.3034686
uniform	11	2	0.036151	0.361668	0.04109869	0.27080928
uniform	13	1	0.034865	0.384298	0.03973342	0.2929247
uniform	13	2	0.037813	0.332311	0.04338325	0.22462803

PLS

hyper parameter	Regression result			
n_components	MSE (training)	R^2 (training)	MSE (validation)	R^2 (validation)
1	**0.026005648**	**0.539848061**	**0.03131058**	**0.400998887**

GPR

hyper parameter			Regression result			
length_scale	nu	alpha	MSE	R^2	MSE	R^2

			(training)	(training)	(validation)	(validation)
1	0.5	1.E-01	0.03834	0.322265	0.04508879	0.19790608
1	1.5	1.E-01	0.028938	0.488482	0.03492742	0.38241803
1	2.5	1.E-01	0.027831	0.507454	0.03337375	0.40758218
10	0.5	1.E-01	0.03834	0.322272	0.04508853	0.1979117
10	1.5	1.E-01	0.028938	0.48848	0.03492757	0.3824165
10	2.5	1.E-01	0.027831	0.507457	0.0333736	0.40758438
100	0.5	1.E-01	0.03834	0.322263	0.04508888	0.19790335
100	1.5	1.E-01	0.028938	0.488477	0.03492766	0.38241386
100	2.5	1.E-01	0.027831	0.507452	0.03337386	0.40758043
1	0.5	1.00E-04	6.37E-07	0.999989	0.02321487	0.6157695
1	1.5	1.00E-04	1.53E-05	0.99973	0.02860897	0.50526657
1	2.5	1.00E-04	2.41E-05	0.999573	0.03163394	0.43355762
10	0.5	1.00E-04	6.38E-07	0.999989	0.02321486	0.61577013
10	1.5	1.00E-04	1.53E-05	0.99973	0.02860914	0.50526491
10	2.5	1.00E-04	3.13E-08	0.999999	0.32026683	-4.9897995
100	0.5	1.00E-04	6.37E-07	0.999989	0.02321487	0.61576938
100	1.5	1.00E-04	3.13E-08	0.999999	0.32026683	-4.9897995
100	2.5	1.00E-04	3.13E-08	0.999999	0.32026683	-4.9897995
1	0.5	1.00E-07	6.68E-13	1	0.02321579	0.61591483
1	1.5	1.00E-07	1.43E-11	1	0.03154317	0.42880763
1	2.5	1.00E-07	2.10E-11	1	0.038532	0.28198275
10	0.5	1.00E-07	6.68E-13	1	0.02321577	0.61591525
10	1.5	1.00E-07	3.13E-13	1	0.25785546	-3.4956761
10	2.5	1.00E-07	3.13E-14	1	0.32026683	-4.9897995
100	0.5	1.00E-07	6.68E-13	1	0.02321583	0.61591401
100	1.5	1.00E-07	3.13E-14	1	0.32026683	-4.9897995
100	2.5	1.00E-07	3.13E-14	1	0.32026683	-4.9897995
1	0.5	1.00E-10	6.68E-19	1	0.02321581	0.61591458
1	1.5	1.00E-10	1.43E-17	1	0.03154836	0.42867936
1	2.5	1.00E-10	2.10E-17	1	0.03853954	0.28185604
10	**0.5**	**1.00E-10**	**6.68E-19**	**1**	**0.0232143**	**0.6159353**
10	1.5	1.00E-10	3.13E-19	1	0.25785548	-3.4956784
10	2.5	1.00E-10	3.13E-20	1	0.32026683	-4.9897995
100	0.5	1.00E-10	6.68E-19	1	0.02321583	0.61591411
100	1.5	1.00E-10	3.13E-20	1	0.32026683	-4.9897995
100	2.5	1.00E-10	3.13E-20	1	0.32026683	-4.9897995

Table S3. 29 descriptors and their evaluation results for 91 different Eu^{2+}-activated phosphors.

num	Phosphor	Space group number	Activator site multiplicity	Activator site symmetry	a/c	b/c	beta	gamma	Volume	Density	CN for A---X	CN for A---A	CN for A---B	CN for A---C	Avg. D A---X	Avg. D A---A	Avg. D A--B	Avg. D A--C	IR of X	IR of A	IR of B	IR of C	Atom N X	Atom N A	Atom N B	Atom N C	Electro negativity X	Electro negativity A	Electro negativity B	Electro negativity C	PEW (eV)	EBEG (eV)	Eg (eV)
1	$Na_2BaSi_2O_6$	4 ($P2_1$)	2	1 (1)	0.42	0.50	91.42	90	308.53	3.61	8	4	3	7	0.3528	0.2317	0.2609	0.2607	1.38	1.42	1.0133	0.26	8	56	11	14	3.44	0.89	0.93	1.9	2.49	2.73	4.17
2	$BaSi_7N_{10}$	7 (Pc)	2	1 (1)	0.70	0.71	106.256	90	425.38	3.7006	13	2	0	20	0.3059	0.2001	0.0000	0.2527	1.46	1.61	0	0.26	7	56	0	14	3.04	0.89	0	1.9	2.61	3.47	3.91
3	$SrSiN_2$	14 ($P2_1/c$)	4	1 (1)	0.75	0.82	113.518	90	221.014	4.319	9	7	0	6	0.3442	0.2654	0.0000	0.2998	1.46	1.31	0	0.26	7	38	0	14	3.04	0.95	0	1.9	1.84	2.09	2.98
4	$MgAl(PO_4)O$	14 ($P2_1/c$)	4	1 (1)	0.53	0.69	98.38	90	397.655814	2.71	5	3	0	6	0.4855	0.2925	0.0000	0.3119	1.38	0.66	0	0.243	8	12	0	14.3333	3.44	1.31	0	1.9966	2.77	2.98	4.98
5	$SrZnP_2O_7$	14 ($P2_1/c$)	4	1 (1)	0.42	0.64	90.1573	90	555.39	3.909	8	2	5	8	0.3815	0.2386	0.2533	0.2667	1.38	1.26	0.68	0.17	8	38	30	15	3.44	0.95	1.65	2.19	2.95	4.40	4.45
6	$BaAl_2Si_2O_8$	15 ($C2/c$)	8	1 (1)	0.60	0.91	115.021	90	1468.049	3.349	10	3	0	12	0.3374	0.2094	0.0000	0.2581	1.38	1.52	0	0.325	8	56	0	13.5	3.44	0.89	0	1.755	2.83	3.20	4.77
7	$BaAl_2Si_2O_8$	15 ($C2/c$)	8	1 (1)	0.60	0.90	115.109	90	1638.87736	3.04	10	3	0	12	0.3368	0.2093	0.0000	0.2579	1.38	1.52	0	0.325	8	56	0	13.5	3.44	0.89	0	1	2.79	3.21	4.78
8	$CaAl_4O_7$	15 ($C2/c$)	4	3 (2)	0.42	0.69	106.75	90	595.08	2.9	7	2	0	12	0.3977	0.2301	0.0000	0.2788	1.38	1.06	0	0.39	8	20	0	13	3.44	1	0	1.755	2.82	3.19	4.00
9	$Ba_2ZnSi_2O_7$	15 ($C2/c$)	8	1 (1)	0.79	0.79	111.3	90	710.75	4.75	8	6	0	10	0.3556	0.2303	0.0000	0.2624	1.38	1.42	0	0.396	8	56	0	19.3333	3.44	0.89	0	1.8166	2.47	2.73	4.00
10	$CaMgSi_2O_6$	15 ($C2/c$)	4	3 (2)	0.54	0.92	105.87	90	439.89	3.27	8	2	0	11	0.4007	0.2258	0.0000	0.2962	1.38	1.12	0	0.3445	8	20	0	12.6667	3.44	1	0	1.51	2.77	3.03	4.95
11	$BaMg_2Si_2O_7$	15 ($C2/c$)	8	1 (1)	0.53	0.92	90.2107	90	1266.44	3.71	9	2	0	17	0.3397	0.2218	0.0000	0.2500	1.38	1.47	0	0.4059	8	56	0	12.5	3.44	0.89	0	1.46	3.08	2.96	4.56
12	$Ba_2MgSi_2O_7$	15 ($C2/c$)	8	1 (1)	0.79	0.79	110.77	90	712.87	4.35	8	6	0	10	0.3549	0.2297	0.0000	0.2624	1.38	1.42	0	0.384	8	56	0	13.3333	3.44	0.89	0	1.7033	2.46	2.71	4.45
13	$SrSiAl_2O_3N_2$	19 ($P2_12_12_1$)	4	1 (1)	0.43	0.70	90	90	450.715	3.6206	9	4	0	14	0.3495	0.2149	0.0000	0.2775	1.4066	1.31	0	0.3436	7.6667	38	0	13.3571	3.3066	0.95	0	1.7135	2.55	2.70	3.72
14	$BaSiAl_2O_3N_2$	19 ($P2_12_12_1$)	4	1 (1)	0.43	0.69	90	90	473.9988	4.1393	9	4	0	14	0.3410	0.2101	0.0000	0.2707	1.4066	1.47	0	0.3436	7.6667	56	0	13.3571	3.3066	0.89	0	1.7135	2.48	2.63	3.71
15	Li_2BaSiO_4	185 ($P6_3cm$)	6	4 (m)	0.76	0.76	90	120	602.8683	4.02	9	4	0	13	0.3423	0.2397	0.0000	0.2778	1.38	1.47	0	0.4631	8	56	0	6.6667	3.44	0.89	0	1.2866	2.44	2.64	4.39
16	$LiSiON$	29 ($Pca2_1$)	4	1 (1)	0.74	0.81	90	90	157.4	2.743	4	6	0	6	0.4900	0.3383	0.0000	0.3210	1.4	0.59	0	0.26	7.75	3	0	14	3.34	0.98	0	1.9	2.59	3.12	5.30
17	$CaAlSiN_3$	36 ($Cmc2_1$)	4	4 (m)	0.52	0.58	90	90	268.72	3.7919	5	2	0	10	0.4035	0.3060	0.0000	0.3098	1.46	1	0	0.325	7	20	0	13.5	3.04	1	0	1.755	1.91	1.97	3.37
18	$BaZn_2Si_2O_7$	36 ($Cmc2_1$)	4	4 (m)	0.52	0.58	90	90	667.264	4.3432	5	2	0	16	0.3668	0.2114	0.0000	0.2483	1.38	1.35	0	0.43	8	56	0	22	3.44	0.89	0	1.775	2.38	2.72	3.26
19	$BaAlSi_4O_3N_3$	36 ($Cmc2_1$)	4	4 (m)	0.43	0.70	90	90	737.6778275	3.3016	11	2	0	14	0.3211	0.2103	0.0000	0.2615	1.416	1.57	0	0.2971	7.5454	56	0	13.7142	3.2581	0.89	0	1.8171	2.61	2.77	3.22
20	$SrAlSiN_3$	36 ($Cmc2_1$)	4	4 (m)	0.53	0.59	90	90	293.53	4.195	5	2	0	10	0.3749	0.2984	0.0000	0.3040	1.46	1.18	0	0.325	7	38	0	13.5	3.04	0.95	0	1.755	2.03	2.15	3.33
21	$MgAlSiN_3$	36 ($Cmc2_1$)	4	4 (m)	0.52	0.58	90	90	249.5641688	3.3107	5	2	0	10	0.4425	0.3230	0.0000	0.3228	1.46	0.66	0	0.274	7	12	0	13.5	3.04	1.31	0	1.755	1.75	2.24	2.19
22	$Sr(Al_{0.3}Si_{0.7})_4(N_{0.8}O_{0.2})_6$	43 ($Fdd2$)	16	1 (1)	0.15	0.25	90	90	2103.4	3.65	10	2	0	13	0.3405	0.2328	0.0000	0.2853	1.4328	1.36	0	0.312	7.2	38	0	13.7	3.12	0.95	0	1.813	2.53	2.86	3.19
23	$BaSi_6N_8O$	44 ($Imm2$)	2	7 ($mm2$)	0.50	0.84	90	90	379.66	3.7955	16	2	0	20	0.2932	0.2067	0.0000	0.2545	1.45	1.61	0	0.26	7.125	56	0	14	3.09	0.89	0	1.9	2.47	3.23	4.29
24	$SrSi_6N_8$	44 ($Imm2$)	2	7 ($mm2$)	0.52	0.85	90	90	349.21	3.5	10	2	0	12	0.3302	0.2083	0.0000	0.2765	1.46	1.36	0	0.26	7	38	0	14	3.04	0.95	0	1.9	2.76	2.85	3.28
25	$BaAlSi_5O_2N_7$	44 ($Imm2$)	2	7 ($mm2$)	0.51	0.85	90	90	390.09	3.7016	16	2	0	20	0.2912	0.2037	0.0000	0.2519	1.44	1.61	0	0.2763	7.125	56	0	13.8333	3.09	0.89	0	1.8516	2.52	3.00	3.70
26	$KMg_4(PO_4)_3$	58 ($Pnnm$)	4	4 (m)	0.38	0.58	90	90	965.4464846	2.898	8	1	6	4	0.3455	0.2504	0.2456	0.3019	1.38	1.51	0.7	0.17	8	19	12	15	3.44	0.82	1.31	2.19	2.79	3.11	4.99
27	$BaSi_2O_2N_2$	60 ($Pbcn$)	4	3 (2)	0.34	0.37	90	90	371.58	4.53	10	4	0	10	0.3360	0.2776	0.0000	0.2516	1.396	1.52	0	0.26	7.8	56	0	14	3.36	0.89	0	1.9	2.51	2.55	3.01
28	$MgSO_4$	62 ($Pnma$)	4	2 ($\bar{1}$)	0.55	0.78	90	90	272.4	2.94	6	2	0	6	0.4766	0.2986	0.0000	0.3059	1.38	0.72	0	0.12	8	12	0	16	3.44	1.31	0	2.58	3.32	3.80	6.00

29	$CaSO_4$	63 (*Cmcm*)	4	7 (*mm*2)	0.90	1.00	90	90	305.37	2.96	8	2	0	6	0.4052	0.2511	0.0000	0.2908	1.38	1.12	0	0.12	8	20	0	16	3.44	1	0	2.58	3.23	3.50	6.21
30	$BaSiN_2$	64 (*Cmca*)	8	4 (*m*)	0.49	0.67	90	90	484.06	5.309	6	7	0	7	0.3488	0.2550	0.0000	0.2854	1.46	1.35	0	0.26	7	56	0	14	3.04	0.89	0	1.9	2.05	2.25	3.01
31	$RbBa(PO_4)$	62 (*Pnma*)	4	4 (*m*)	0.57	0.78	90	90	450.92	4.68	9	4	6	6	0.3504	0.2243	0.2521	0.2575	1.38	1.47	1.69	0.17	8	56	37	15	3.44	0.89	0.82	2.19	2.88	2.98	5.00
32	$BaSO_4$	62 (*Pnma*)	4	4 (*m*)	0.61	0.81	90	90	344.77	4.5	12	8	0	7	0.3417	0.2137	0.0000	0.2736	1.38	1.61	0	0.12	8	56	0	16	3.44	0.89	0	2.58	3.32	3.75	5.97
33	$SrB_2Si_2O_8$	62 (*Pnma*)	4	4 (*m*)	0.89	0.91	90	90	576.0392	4	10	4	0	12	0.3532	0.2069	0.0000	0.2825	1.38	1.36	0	0.115	8	38	0	9.5	3.44	0.95	0	1.97	2.85	2.93	5.49
34	$BaB_2Si_2O_8$	62 (*Pnma*)	4	4 (*m*)	0.90	0.90	90	90	606	4	10	4	0	12	0.3468	0.2036	0.0000	0.2785	1.38	1.52	0	0.115	8	56	0	9.5	3.44	0.89	0	1.97	3.06	3.19	5.54
35	$SrSO_4$	62 (*Pnma*)	4	4 (*m*)	0.64	0.82	90	90	306.45335	3.97	12	8	0	7	0.3543	0.2228	0.0000	0.2799	1.38	1.44	0	0.12	8	38	0	16	3.44	0.95	0	2.58	3.31	3.61	5.93
36	$Sr[Mg_2Al_2N_4]$	87 (*I*4/*m*)	2	11 (4/*m*)	0.41	1.00	90	90	218.32	3.75	8	2	0	12	0.3554	0.3006	0.0000	0.3063	1.46	1.26	0	0.48	7	38	0	12.5	3.04	0.95	0	1.46	2.03	2.04	1.93
37	$Sr_8(Si_4O_{12})Cl_8$	87 (*I*4/*m*)	16	1 (1)	0.85	1.00	90	90	1190.008075	3.5971	9	6	0	2	0.3420	0.2417	0.0000	0.3006	1.6188	1.31	0	0.26	11.6	38	0	14	3.328	0.95	0	1.9	2.55	2.78	5.13
38	$Ca[LiAl_3N_4]$	88 ($I4_1/a$)	16	1 (1)	0.87	0.87	90	90	1602.3	3.051	8	2	0	12	0.3669	0.3099	0.0000	0.3140	1.46	1.12	0	0.44	7	20	0	10.5	3.04	1	0	1.4525	1.86	2.00	3.02
39	$Sr[Mg_3SiN_4]$	88 ($I4_1/a$)	16	1 (1)	0.85	0.85	90	90	1785.4	3.641	12	10	0	12	0.3154	0.1827	0.0000	0.3030	1.46	1.26	0	0.4925	7	38	0	12.5	3.04	0.95	0	1.4575	2.02	2.07	3.01
40	BaB_8O_{13}	91 ($P4_122$)	4	3 (2)	0.65	0.65	90	90	967.21	2.97	12	10	0	18	0.3292	0.1461	0.0000	0.2595	1.38	1.61	0	0.11	8	56	0	5	3.44	0.89	0	2.04	3.04	3.20	5.55
41	$Ca_2Al_2SiO_7$ ($Ca_2Al_{1.77}Si_{1.23}O_{6.77}N_{0.23}$)	113 ($P\text{-}42_1m$)	4	4 (*m*)	0.66	1.00	90	90	296.924	3.0669	8	1	0	10	0.3965	0.2858	0.0000	0.2805	1.3823	1.12	0	0.351	7.9671	20	0	13.3	3.4268	1	0	1.697	2.37	2.53	4.31
42	$SrCaSiAl_2O_7$	113 ($P\text{-}42_1m$)	4	4 (*m*)	0.66	1.00	90	90	309.346	3.4542	8	1	0	10	0.3773	0.2915	0.0000	0.2735	1.38	1.19	0	0.351	8	29	0	13.3	3.44	0.975	0	1.697	2.34	2.50	4.16
43	$Sr_2Al_{1.6}Si_{1.4}O_{6.6}N_{0.4}$	113 ($P\text{-}42_1m$)	4	4 (*m*)	0.67	1.00	90	90	323.31	3.83	8	1	0	10	0.3741	0.2815	0.0000	0.2720	1.3848	1.26	0	0.3328	7.9428	38	0	13.3333	3.4171	0.95	0	1.7066	2.55	2.40	4.06
44	$Sr_2ZnSi_2O_7$	113 ($P\text{-}42_1m$)	4	4 (*m*)	0.65	1.00	90	90	331.0787312	4.0978	8	1	0	10	0.3746	0.2673	0.0000	0.2712	1.38	1.26	0	0.396	8	38	0	19.3333	3.44	0.95	0	1.8166	2.61	3.11	3.93
45	$Ca_2MgSi_2O_7$	113 ($P\text{-}42_1m$)	4	4 (*m*)	0.63	1.00	90	90	307.55	2.95	8	1	0	10	0.3885	0.2692	0.0000	0.2763	1.38	1.12	0	0.384	8	20	0	13.3333	3.44	1	0	1.7033	2.39	2.75	4.51
46	$Sr_2MgSi_2O_7$	113 ($P\text{-}42_1m$)	4	4 (*m*)	0.64	1.00	90	90	335.8704666	3.636	8	1	0	10	0.3758	0.2674	0.0000	0.2720	1.38	1.26	0	0.384	8	38	0	13.3333	3.44	0.95	0	1.7033	2.30	2.77	4.54
47	$SrLaGa_3S_6O$	113 ($P\text{-}42_1m$)	4	4 (*m*)	0.65	1.00	90	90	535.0782145	3.9997	8	1	0	10	0.3353	0.2470	0.0000	0.2316	1.7825	1.21	0	0.47	14.8571	47.5	0	31	2.7028	1.025	0	1.81	2.30	2.37	2.55
48	Li_2CaSiO_4	121 (*I*-42*m*)	2	14 ($\bar{4}2m$)	0.78	0.78	90	90	165.21	2.94	8	12	0	14	0.3931	0.2042	0.0000	0.3128	1.38	1.12	0	0.4486	8	20	0	6.6667	3.44	1	0	1.2866	2.58	2.56	5.49
49	$KSrBP_2O_8$	122 (*I*-42*d*)	8	3 (2)	0.51	0.51	90	90	701.7	3.1	8	2	0	8	0.3569	0.2462	0.0000	0.2746	1.38	1.385	0	0.155	8	28.5	0	11.6667	3.44	0.885	0	2.14	2.73	3.00	5.23
50	$KBaBP_2O_8$	122 (*I*-42*d*)	8	3 (2)	0.50	0.50	90	90	741.7	3.378	8	2	0	8	0.3481	0.2445	0.0000	0.2682	1.38	1.465	0	0.155	8	37.5	0	11.6667	3.44	0.855	0	2.14	2.67	2.97	4.81
51	$BaMgSi_4O_{10}$	130 (*P*4/*ncc*)	4	10 ($\bar{4}$)	0.47	0.47	90	90	903.039456	3.19	8	4	4	8	0.3540	0.1888	0.2490	0.2737	1.38	1.42	0.57	0.26	8	56	12	14	3.44	0.89	1.31	1.9	2.76	2.82	4.42
52	$Sr_3GdNa(PO_4)_3F$	147 (*P*-3)	6	1 (1)	0.74	1.00	90	120	564.795	4.3925	10	6	4	5	0.3579	0.2372	0.2441	0.2828	1.373	1.36	1.0635	0.17	8.0769	38	37.5	15	3.4815	0.95	1.065	2.19	2.64	2.83	3.24
53	$BaAl_2Si_2O_8$	147 (*P*-3)	1	17 ($\bar{3}$)	0.68	0.68	90	120	189.127	3.297	12	6	0	12	0.3211	0.1888	0.0000	0.2634	1.38	1.61	0	0.325	8	56	0	13.5	3.44	0.89	0	1.755	3.33	3.48	4.94
54	$SrSi_9Al_{19}ON_{31}$	148 (*R*-3)	3	17 ($\bar{3}$)	0.07	0.07	90	120	1949.735687	3.3332	12	6	0	12	0.3298	0.1874	0.0000	0.2796	1.4575	1.44	0	0.3482	7.0312	38	0	13.3214	3.0525	0.95	0	1.7032	2.63	2.89	1.84
55	Li_2SrSiO_4	152 ($P3_121$)	3	3 (2)	0.40	0.40	90	120	272.1887873	3.54	8	12	0	14	0.3801	0.1974	0.0000	0.3022	1.38	1.26	0	0.4486	8	38	0	6.6667	3.44	0.95	0	1.2866	2.21	2.39	4.65
56	$SrBPO_5$	154 ($P3_221$)	3	3 (2)	1.00	1.00	90	120	282.03	3.7	10	4	0	10	0.3667	0.2315	0.0000	0.2798	1.38	1.36	0	0.146	8	38	0	11	3.44	0.95	0	2.13	2.84	3.01	5.39
57	Ca-a-SiAlON ($Ca_{0.375}Si_{11.25}Al_{0.75}N_{16}$)	159 (*P*31*c*)	2	16 (3)	0.73	1.00	90	120	297.3119177	3.1384	11	8	0	12	0.3570	0.1852	0.0000	0.3192	1.46	1.285	0	0.2837	7	20	0	13.9375	3.04	1	0	1.8818	2.13	2.33	3.44
58	Sr-a-SiAlON ($Sr_{0.375}Si_{11.25}Al_{0.75}N_{16}$)	159 (*P*31*c*)	2	16 (3)	0.73	1.00	90	120	297.2721148	3.2376	11	8	0	12	0.3559	0.1852	0.0000	0.3191	1.46	1.4	0	0.2779	7	38	0	13.9375	3.04	0.95	0	1.8818	2.16	2.34	1.77
59	$LiCaPO_4$	159 (*P*31*c*)	6	1 (1)	0.76	0.76	90	120	488.6710363	2.89	8	4	0	6	0.3940	0.2648	0.0000	0.2987	1.38	1.12	0	0.24	8	20	0	9	3.44	1	0	1.585	2.64	2.71	5.18
60	$BaAlBO_3F_2$	174 (*P*-6)	2	16 (3)	0.52	0.52	90	120	193.26	4.49	12	8	0	12	0.3454	0.2070	0.0000	0.2728	1.345	1.61	0	0.25	8.4	56	0	9	3.656	0.89	0	1.825	2.76	2.83	6.06

61	$CaZrBAl_9O_{18}$	173 ($P6_3$)	2	17 ($\bar{3}$)	0.97	1.00	90	120	557.74	4.007	6	10	6	18	0.4170	0.1287	0.1832	0.2457	1.38	1.12	0.59	0.2967	8	20	40	10.3333	3.44	1	1.33	1.7533	2.85	3.39	4.89
62	$SrYSi_4N_7$	186 ($P6_3mc$)	2	19 (3m)	0.61	0.61	90	120	306.83	4.188	12	12	4	12	0.3320	0.1664	0.2718	0.2851	1.46	1.44	0.9	0.26	7	38	39	14	3.04	0.95	1.22	1.9	2.24	2.79	2.76
63	$CaScSi_4N_7$	186 ($P6_3mc$)	2	19 (3m)	0.61	0.61	90	120	288.98	3.3951	12	12	4	12	0.3393	0.1698	0.2772	0.2904	1.46	1.34	0.745	0.26	7	20	21	14	3.04	1	1.36	1.9	2.37	2.73	2.88
64	$SrScSi_4N_7$	186 ($P6_3mc$)	2	19 (3m)	0.61	0.61	90	120	292.24	3.894	12	12	4	12	0.3383	0.1692	0.2764	0.2895	1.46	1.44	0.745	0.26	7	38	21	14	3.04	0.95	1.36	1.9	2.40	2.73	2.96
65	$BaScSi_4N_7$	186 ($P6_3mc$)	2	19 (3m)	0.61	0.61	90	120	297.63	4.3816	12	12	4	12	0.3360	0.1681	0.2745	0.2876	1.46	1.61	0.745	0.26	7	56	21	14	3.04	0.89	1.36	1.9	2.38	2.67	2.91
66	$BaZrSi_3O_9$	188 (P-6c2)	2	18 (32)	0.68	0.68	90	120	395.841	3.8325	6	2	3	6	0.3598	0.1999	0.2563	0.2635	1.38	1.35	0.59	0.26	8	56	40	14	3.44	0.89	1.33	1.9	2.61	2.70	4.66
67	$BaHfSi_3O_9$	188 (P-6c2)	2	18 (32)	0.68	0.68	90	120	397.48	4.5459	6	2	3	6	0.3567	0.1999	0.2557	0.2654	1.38	1.35	0.58	0.26	8	56	72	14	3.44	0.89	1.3	1.9	2.61	2.74	4.69
68	$Mg_2Al_4Si_5O_{18}$	192 ($P6/mcc$)	4	18 (32)	0.95	1.00	90	120	775.7	2.5044	6	2	0	9	0.4716	0.2144	0.0000	0.3042	1.38	0.72	0	0.3163	8	12	0	13.5555	3.44	1.31	0	1.7711	2.72	2.94	4.13
69	Sr_2ScAlO_5	205 (Pa-3)	8	16 (3)	1.00	1.00	90	90	494.5008364	4.27	12	6	0	8	0.3566	0.2528	0.0000	0.2920	1.38	1.44	0	0.4788	8	38	0	17	3.44	0.95	0	1.485	2.02	2.16	3.13
70	$Sr_8Al_{12}O_{24}S_2$	217 (I-43m)	8	19 (3m)	1.00	1.00	90	90	793.2512976	3.083	4	9	0	6	0.3856	0.2041	0.0000	0.2909	1.495	1.18	0	0.39	8.6153	38	0	13	3.3738	0.95	0	1.61	2.05	2.20	3.34
71	$Sr_3Bi(PO_4)_3$	220 (I-43d)	16	16 (3)	1.00	1.00	90	90	1062.300795	4.732	6	3	0	6	0.4164	0.2572	0.0000	0.2830	1.38	1.1425	0	0.17	8	49.25	0	15	3.44	1.2175	0	2.19	2.93	3.08	3.94
72	$Sr_{12}Al_{14}O_{32}Cl_2$	220 (I-43d)	24	3 (2)	1.00	1.00	90	90	1882.35	3.55	7	4	0	7	0.3750	0.2637	0.0000	0.2853	1.403	1.21	0	0.39	8.5294	38	0	13	3.4235	0.95	0	1.61	2.37	2.85	3.58
73	$Ca_{12}Al_{14}O_{32}Cl_2$	220 (I-43d)	24	3 (2)	1.00	1.00	90	90	1732.11	2.74	7	4	0	7	0.4005	0.2713	0.0000	0.2935	1.4414	1.06	0	0.39	8.5294	20	0	13	3.4235	1	0	1.61	2.81	3.10	3.75
74	$CsAlSi_2O_6$	230 (Ia-3d)	16	18 (32)	1.00	1.00	90	90	2593.94	3.2	12	3	0	9	0.2809	0.2058	0.0000	0.2483	1.38	1.88	0	0.303	8	55	0	13.6667	3.44	0.79	0	1.8033	2.78	3.13	4.11
75	$Ba_2LiB_5O_{10}$	11 ($P2_1/m$)	4	1 (1)	0.30	0.46	104.26	90	417.6	3.941	12	6	0	11	0.3252	0.2242	0.0000	0.2801	1.38	1.61	0	0.197	8	56	0	4.6667	3.44	0.89	0	1.8633	2.11	3.00	4.93
76	$BaAl_2B_2O_7$	155 (R32)	3	18 (32)	0.21	0.21	90	120	528.01	3.07	6	6	0	12	0.3642	0.2000	0.0000	0.2812	1.358571429	1.35	0	0.2	8	56	0	9	3.44	0.89	0	1.825	3.31	3.45	4.65
77	$BaBeSiO_4$	8 (Cm)	2	4 (m)	0.58	0.58	55.575	90	191.61	4.13	12	12	0	10	0.3310	0.1947	0.0000	0.2908	1.38	1.47	0	0.265	8	56	0	9	3.44	0.89	0	1.735	2.69	3.05	4.77
78	$BaGa_2SiS_6$	146 (R3)	3	16 (3)	0.91	1.00	90	120	683.82	3.62	12	6	0	9	0.2827	0.1607	0.0000	0.2368	1.84	1.61	0	0.365	16	56	0	25.333	2.58	0.89	0	1.84	2.44	2.67	3.00
79	$BaMg_3SiN_4$	2 (P-1)	1	2 ($\bar{1}$)	0.57	0.99	73.697	73.566	117.6	4.16	8	2	0	12	0.3387	0.2898	0.0000	0.2982	1.46	1.42	0	0.4925	7	56	0	12.5	3.04	0.89	0	1.4575	1.82	2.09	1.82
80	$BaMgP_2O_7$	14 ($P2_1/c$)	4	1 (1)	0.43	0.68	91.32	90	592.51	3.76	10	2	0	13	0.3454	0.2263	0.0000	0.2596	1.35571	1.42	0.72	0.17	8	56	12	15	3.44	0.89	1.31	2.19	3.06	3.27	5.32
81	$CsMgPO_4$	62 ($Pnma$)	4	4 (m)	0.57	0.93	90	90	476.43	3.52	15	4	0	12	0.2799	0.2138	0.0000	0.2521	1.38	1.74	0	0.37	8	55	0	35	3.44	0.79	0	1.05	1.96	2.74	4.42
82	$LiSrPO_4$	170 ($P6_5$)	6	1 (1)	0.20	0.20	90	120	534.15	3.54	8	2	0	12	0.3751	0.2435	0.0000	0.2805	1.375	1.21	0	0.38	8	38	0	9.5	3.44	0.95	0	1.585	2.77	2.81	5.18
83	$RbLi(Li_3SiO_4)_2$	12 ($C2/m$)	4	4 (m)	0.41	0.50	90.53	90	770.98	2.74	8	2	0	12	0.3344	0.3107	0.0000	0.2957	1.393333333	1.61	0	0.516667	8	37	0	4.66667	3.44	0.82	0	1.184444	2.34	2.39	4.72
84	$Sr_2Al_2SiO_7$	113 (P-42$_1m$)	4	4 (m)	0.67	1.00	90	90	321.91	3.81	8	1	0	10	0.3752	0.2794	0.0000	0.2718	1.38	1.26	0	0.34666666	8	38	0	13.33333	3.44	0.95	0	1.706667	2.35	2.67	4.06
85	$Sr_4LiAl_{11}N_{14}$	58 ($Pnnm$)	4	4 (m)	0.31	1.00	90	90	351.91	4.01	8	2	0	11	0.3595	0.3091	0.0000	0.3067	1.46	1.26	0	0.406666667	7	38	0	12.08333	3.04	0.95	0	1.5575	1.86	1.97	2.07
86	$SrAl_4O_7$	15 ($C2/c$)	4	3 (2)	0.42	0.69	106.7	90	623.01	3.28	7	8	0	12	0.3826	0.1772	0.0000	0.2733	1.38	1.26	0	0.39	8	38	0	13	3.44	0.95	0	1.61	2.56	3.02	3.75
87	SrB_4O_7	31 ($Pmn2_1$)	2	4 (m)	0.40	0.41	90	90	201	4.01	16	4	0	18	0.3446	0.2307	0.0000	0.2879	1.37142857	1.31	0	0.11	8	38	0	5	3.44	0.95	0	2.04	3.32	3.45	7.30
88	$BaSi_2O_5$	62 ($Pnma$)	4	4 (m)	0.34	0.57	90	90	481.51	3.77	9	6	0	4	0.3427	0.2155	0.0000	0.2863	1.368	1.47	0	0.26	8	38	0	14	3.44	0.95	0	1.9	2.49	3.10	4.79
89	$CdSrP_2O_7$	14 ($P2_1/c$)	4	1 (1)	0.42	0.67	90.01	90	600.65	4.14	8	2	4	7	0.3794	0.2299	0.2520	0.2691	1.36714285	1.26	1.03	0.17	8	38	48	15	3.44	0.95	1.69	2.19	2.96	3.04	3.70
90	$Sr_3NaY(PO_4)_3F$	147 (P-3)	6	1 (1)	0.74	1.00	90	120	562.86	4	8	6	6	7	0.3819	0.2379	0.1784	0.2713	1.37125	1.26	1.18	0.412571429	8.125	38	11	21.85714286	3.5075	0.95	0.93	1.912857143	2.65	2.84	5.35
91	$SrMgAl_{10}O_{17}$	194 ($P6_3/mmc$)	2	26 ($\bar{6}m2$)	0.25	0.25	90	120	613.17	3.54	6	6	0	12	0.3796	0.1777	0.0000	0.2784	1.368823529	1.18	0	0.505227273	8	38	0	12.90909	3.44	0.95	0	1.582727	2.56	2.92	4.36

Table S4a. The training, validation and hold-out dataset test results for (a) EBEW prediction model in terms of MSE and R^2 using two data-splitting schemes: 9-cross-validation and 8-fold cross-validation with a holdout test dataset.

EBEW

	9-Fold Cross Validation				8-Fold Cross Validation with Hold-Out Dataset Test					
ML algorithm	MSE (training)	R^2 (training)	MSE (validation)	R^2 (validation)	MSE (training)	R^2 (training)	MSE (validation)	R^2 (validation)	MSE (test)	R^2 (test)
Basic linear	0.006	0.80	0.015	0.50	0.006	0.82	0.016	0.44	0.018	0.49
Ridge	0.008	0.75	0.013	0.60	0.008	0.75	0.013	0.59	0.012	0.65
Lasso	0.009	0.73	0.013	0.58	0.008	0.74	0.014	0.55	0.013	0.62
LARS	0.010	0.68	0.014	0.55	0.010	0.69	0.014	0.53	0.013	0.62
Elastic net	0.008	0.76	0.013	0.59	0.008	0.76	0.014	0.55	0.013	0.63
KRR	0.010	0.69	0.013	0.59	0.010	0.69	0.013	0.55	0.012	0.64
BRR	0.008	0.75	0.012	0.60	0.008	0.76	0.013	0.59	0.012	0.65
ARD	0.008	0.75	0.013	0.58	0.008	0.76	0.014	0.53	0.014	0.59
Random Forest	0.002	0.93	0.015	0.52	0.002	0.93	0.015	0.52	0.016	0.55
Ada Boost	0.006	0.83	0.017	0.46	0.005	0.84	0.016	0.49	0.014	0.59
Gradient Boost	0.004	0.88	0.014	0.57	0.004	0.88	0.015	0.53	0.013	0.62
XG Boost	0.001	0.98	0.016	0.48	0.001	0.98	0.015	0.51	0.014	0.59
SVR	0.008	0.74	0.012	0.60	0.008	0.75	0.013	0.56	0.014	0.61
KNN	0.000	1.00	0.018	0.41	0.000	1.00	0.018	0.39	0.016	0.53
PLS	0.016	0.51	0.019	0.35	0.016	0.51	0.020	0.36	0.019	0.46
GPR	0.000	1.00	0.014	0.56	0.000	1.00	0.013	0.60	0.013	0.63
Average	0.007	0.80	0.014	0.53	0.006	0.80	0.015	0.519	0.014	0.59

Table S4b. The training, validation and hold-out dataset test results for (b) E_g prediction model in terms of MSE and R^2 using two data-splitting schemes: 9-cross-validation and 8-fold cross-validation with a holdout test dataset.

Eg

ML algorithm	9-Fold Cross Validation				8-Fold Cross Validation with Hold-Out Dataset Test					
	MSE (training)	R^2 (training)	MSE (validation)	R^2 (validation)	MSE (training)	R^2 (training)	MSE (validation)	R^2 (validation)	MSE (test)	R^2 (test)
Basic linear	0.006	0.83	0.016	0.50	0.006	0.82	0.025	0.18	0.042	0.14
Ridge	0.008	0.78	0.014	0.62	0.008	0.77	0.015	0.56	0.018	0.63
Lasso	0.008	0.78	0.013	0.64	0.008	0.78	0.014	0.54	0.018	0.64
LARS	0.009	0.75	0.013	0.65	0.009	0.75	0.013	0.61	0.019	0.60
Elastic net	0.008	0.79	0.013	0.62	0.007	0.79	0.013	0.64	0.020	0.60
KRR	0.011	0.71	0.015	0.60	0.011	0.70	0.015	0.58	0.020	0.59
BRR	0.008	0.80	0.014	0.61	0.008	0.79	0.014	0.60	0.019	0.60
ARD	0.008	0.78	0.015	0.58	0.008	0.77	0.013	0.58	0.019	0.60
Random Forest	0.002	0.95	0.013	0.63	0.002	0.94	0.014	0.60	0.017	0.66
Ada Boost	0.005	0.86	0.013	0.60	0.004	0.88	0.014	0.58	0.019	0.60
Gradient Boost	0.002	0.94	0.014	0.61	0.002	0.95	0.013	0.61	0.016	0.68
XG Boost	0.000	0.99	0.013	0.62	0.000	0.99	0.015	0.53	0.019	0.61
SVR	0.008	0.78	0.013	0.57	0.008	0.77	0.014	0.51	0.018	0.64
KNN	0.000	1.00	0.019	0.48	0.000	1.00	0.019	0.47	0.021	0.57
PLS	0.015	0.60	0.019	0.46	0.014	0.62	0.020	0.40	0.027	0.46
GPR	0.000	1.00	0.014	0.63	0.000	1.00	0.015	0.58	0.018	0.63
Average	0.006	0.83	0.014	0.59	0.006	0.83	0.015	0.536	0.021	0.58

Table S5a. The training and validation results for (a) PEW prediction models in terms of MSE for leave-one-out cross-validation with no holdout test dataset. Note that R^2 is unavailable for the leave-one-out cross-validation scheme.

PEW

	Leave-one-out Cross Validation	
ML algorithm	MSE (training)	MSE (validation)
Basic linear	0.012	0.028
Ridge	0.014	0.022
Lasso	0.014	0.023
LARS	0.016	0.022
Elastic net	0.013	0.022
KRR	0.016	0.022
BRR	0.013	0.022
ARD	0.014	0.022
Random Forest	0.004	0.025
Ada Boost	0.013	0.028
Gradient Boost	0.006	0.026
XG Boost	0.001	0.03
SVR	0.014	0.02
KNN	0	0.029
PLS	0.026	0.034
GPR	0	0.023

Table S5b. The training and validation results for (b) EBEW prediction models in terms of MSE for leave-one-out cross-validation with no holdout test dataset. Note that R^2 is unavailable for the leave-one-out cross-validation scheme.

EBEW

	Leave-one-out Cross Validation	
ML algorithm	MSE (training)	MSE (validation)
Basic linear	0.007	0.015
Ridge	0.008	0.013
Lasso	0.009	0.014
LARS	0.011	0.015
Elastic net	0.008	0.013
KRR	0.010	0.013
BRR	0.008	0.013
ARD	0.008	0.014
Random Forest	0.002	0.016
Ada Boost	0.007	0.018
Gradient Boost	0.004	0.014
XG Boost	0.001	0.018
SVR	0.009	0.013
KNN	0.000	0.018
PLS	0.016	0.021
GPR	0.000	0.014

Table S5c. The training and validation results for (c) E_g prediction model in terms of MSE for leave-one-out cross-validation with no holdout test dataset. Note that R^2 is unavailable for the leave-one-out cross-validation scheme.

Eg		
	Leave-one-out Cross Validation	
ML algorithm	MSE (training)	MSE (validation)
Basic linear	0.007	0.019
Ridge	0.008	0.015
Lasso	0.009	0.014
LARS	0.010	0.014
Elastic net	0.008	0.014
KRR	0.011	0.015
BRR	0.008	0.015
ARD	0.008	0.017
Random Forest	0.002	0.014
Ada Boost	0.006	0.014
Gradient Boost	0.003	0.015
XG Boost	0.001	0.016
SVR	0.008	0.015
KNN	0.000	0.020
PLS	0.015	0.021
GPR	0.000	0.015

Table S6a. Over-fitting index for (a) PEW prediction model in terms of Training_MSE/Validation_MSE, Validation_R^2/Training_R^2, Training_MSE/Test_MSE and Test_R^2/Training_R^2 for 9- and 8-fold cross validations.

PEW

	Overfitting Index					
	9-Fold Cross Validation		8-Fold Cross Validation with Hold-Out Dataset Test			
ML algorithm	MSE_tr/val	R^2_val/tr	MSE_tr/val	R^2_val/tr	MSE_tr/te	R^2_te/tr
Basic linear	0.43	0.59	0.39	0.51	0.33	0.48
Ridge	0.63	0.81	0.61	0.78	0.66	0.81
Lasso	0.62	0.79	0.57	0.75	0.70	0.82
LARS	0.71	0.84	0.67	0.77	0.71	0.82
ENR	0.60	0.78	0.52	0.66	0.71	0.85
KRR	0.77	0.87	0.76	0.85	0.90	0.92
BRR	0.60	0.79	0.59	0.77	0.65	0.80
ARD	0.66	0.81	0.56	0.73	0.69	0.82
Random Forest	0.15	0.63	0.15	0.57	0.16	0.58
Ada Boost	0.52	0.71	0.42	0.55	0.61	0.79
Gradient Boost	0.20	0.64	0.15	0.52	0.14	0.51
XG Boost	0.04	0.54	0.03	0.51	0.03	0.46
SVR	0.66	0.82	0.57	0.75	0.77	0.88
KNN	0.00	0.48	0.00	0.45	0.00	0.32
PLS	0.83	0.74	0.82	0.80	0.81	0.74
GPR	0.00	0.62	0.00	0.61	0.00	0.52

Table S6b. Over-fitting index for (b) EBEW model in terms of Training_MSE/Validation_MSE, Validation_R^2/Training_R^2, Training_MSE/Test_MSE and Test_R^2/Training_R^2 for 9- and 8-fold cross validations.

EBEW

Overfitting Index						
	9-Fold Cross Validation		8-Fold Cross Validation with Hold-Out Dataset Test			
ML algorithm	MSE_tr/val	R^2_val/tr	MSE_tr/val	R^2_val/tr	MSE_tr/te	R^2_te/tr
Basic linear	0.43	0.62	0.34	0.54	0.32	0.59
Ridge	0.65	0.80	0.62	0.78	0.66	0.86
Lasso	0.67	0.79	0.61	0.74	0.63	0.84
LARS	0.72	0.81	0.71	0.77	0.74	0.89
ENR	0.63	0.78	0.56	0.72	0.59	0.82
KRR	0.80	0.86	0.75	0.80	0.80	0.93
BRR	0.65	0.80	0.61	0.78	0.64	0.85
ARD	0.62	0.76	0.56	0.69	0.56	0.78
Random Forest	0.16	0.56	0.14	0.56	0.14	0.59
Ada Boost	0.33	0.56	0.32	0.59	0.36	0.70
Gradient Boost	0.28	0.64	0.27	0.61	0.30	0.71
XG Boost	0.04	0.49	0.04	0.52	0.05	0.60
SVR	0.68	0.81	0.65	0.76	0.60	0.81
KNN	0.00	0.41	0.00	0.39	0.00	0.53
PLS	0.83	0.70	0.78	0.71	0.84	0.89
GPR	0.00	0.56	0.00	0.60	0.00	0.63

Table S6c. Over-fitting index for (c) E_g prediction model in terms of Training_MSE/Validation_MSE, Validation_R^2/Training_R^2, Training_MSE/Test_MSE and Test_R^2/Training_R^2 for 9- and 8-fold cross validations.

Eg

Overfitting Index						
	9-Fold Cross Validation		8-Fold Cross Validation with Hold-Out Dataset Test			
ML algorithm	MSE_tr/val	R^2_val/tr	MSE_tr/val	R^2_val/tr	MSE_tr/te	R^2_te/tr
Basic linear	0.39	0.60	0.25	0.22	0.15	0.17
Ridge	0.59	0.80	0.54	0.73	0.43	0.81
Lasso	0.63	0.82	0.54	0.69	0.44	0.82
LARS	0.72	0.87	0.67	0.80	0.45	0.80
ENR	0.59	0.79	0.56	0.81	0.38	0.76
KRR	0.73	0.84	0.71	0.82	0.52	0.84
BRR	0.53	0.76	0.53	0.76	0.39	0.77
ARD	0.54	0.74	0.61	0.76	0.43	0.78
Random Forest	0.16	0.67	0.15	0.63	0.12	0.70
Ada Boost	0.40	0.70	0.30	0.67	0.22	0.69
Gradient Boost	0.15	0.64	0.13	0.65	0.11	0.72
XG Boost	0.04	0.62	0.03	0.53	0.02	0.62
SVR	0.59	0.73	0.56	0.66	0.45	0.83
KNN	0.00	0.48	0.00	0.47	0.00	0.57
PLS	0.80	0.77	0.69	0.65	0.51	0.74
GPR	0.00	0.63	0.00	0.58	0.00	0.63

Table S7a. Summary of the surrogate ML model regression results for (a) PEW prediction model. The training, validation and test results in terms of MSE, R^2, and over-fitting index for 8-fold cross validation with a holdout dataset test.

PEW

	9-Feature Surrogate Model (8-Fold Cross Validation with Hold-Out Dataset Test)						Overfitting Index	
ML algorithm	MSE (training)	R^2 (training)	MSE (validation)	R^2 (validation)	MSE (test)	R^2 (test)	MSE_tr/val	R^2_val/tr
Basic linear	0.031	0.44	0.056	0.02	0.021	0.61	0.56	0.05
Ridge	0.035	0.38	0.042	0.20	0.029	0.45	0.82	0.53
Lasso	0.034	0.40	0.042	0.22	0.048	0.09	0.80	0.55
LARS	0.034	0.39	0.040	0.27	0.029	0.46	0.85	0.69
ENR	0.033	0.41	0.044	0.16	0.031	0.42	0.76	0.40
KRR	0.039	0.30	0.047	0.10	0.049	0.08	0.83	0.33
BRR	0.034	0.39	0.044	0.18	0.028	0.48	0.78	0.46
ARD	0.035	0.38	0.041	0.25	0.036	0.32	0.85	0.65
Random Forest	0.007	0.88	0.040	0.21	0.028	0.48	0.17	0.24
Ada Boost	0.022	0.61	0.039	0.26	0.032	0.40	0.56	0.42
Gradient Boost	0.010	0.82	0.034	0.37	0.035	0.34	0.30	0.45
XG Boost	0.004	0.94	0.041	0.26	0.034	0.35	0.09	0.28
SVR	0.034	0.39	0.044	0.17	0.028	0.48	0.77	0.44
KNN	0.000	1.00	0.048	0.13	0.021	0.60	0.00	0.13
PLS	0.038	0.32	0.044	0.14	0.054	-0.02	0.87	0.43
GPR	0.000	1.00	0.041	0.19	0.049	0.08	0.00	0.19

Table S7b. Summary of the surrogate ML model regression results for (b) EBEW prediction model. The training, validation and test results in terms of MSE, R^2, and over-fitting index for 8-fold cross validation with a holdout dataset test. The negative R^2 could be regarded as a regression failure.

EBEW

	9-Feature Surrogate Model (8-Fold Cross Validation with Hold-Out Dataset Test)						Overfitting Index	
ML algorithm	MSE (training)	R^2 (training)	MSE (validation)	R^2 (validation)	MSE (test)	R^2 (test)	MSE_tr/val	R^2_val/tr
Basic linear	0.018	0.42	0.045	-1.58	0.019	0.46	0.41	-3.73
Ridge	0.020	0.36	0.023	0.28	0.028	0.18	0.88	0.78
Lasso	0.020	0.37	0.024	0.27	0.027	0.21	0.86	0.72
LARS	0.020	0.36	0.023	0.30	0.028	0.20	0.90	0.83
ENR	0.020	0.38	0.023	0.27	0.026	0.24	0.85	0.71
KRR	0.029	0.07	0.039	-0.14	0.019	0.46	0.76	-1.90
BRR	0.020	0.37	0.023	0.28	0.028	0.19	0.87	0.75
ARD	0.019	0.40	0.021	0.34	0.023	0.33	0.92	0.85
Random Forest	0.004	0.88	0.023	0.25	0.022	0.36	0.16	0.28
Ada Boost	0.014	0.57	0.021	0.33	0.023	0.33	0.65	0.58
Gradient Boost	0.010	0.69	0.020	0.42	0.019	0.44	0.51	0.61
XG Boost	0.002	0.94	0.023	0.07	0.023	0.33	0.09	0.07
SVR	0.020	0.38	0.022	0.30	0.024	0.30	0.90	0.78
KNN	0.000	1.00	0.030	0.00	0.017	0.52	0.00	0.00
PLS	0.023	0.29	0.024	0.22	0.032	0.08	0.93	0.75
GPR	-	-	-	-	-	-	-	-

Table S7c. Summary of the surrogate ML model regression results for (c) E_g prediction model. The training, validation and test results in terms of MSE, R^2, and over-fitting index for 8-fold cross validation with a holdout dataset test. The negative R^2 could be regarded as a regression failure.

Eg

	9-Feature Surrogate Model (8-Fold Cross Validation with Hold-Out Dataset Test)						Overfitting Index	
ML algorithm	MSE (training)	R^2 (training)	MSE (validation)	R^2 (validation)	MSE (test)	R^2 (test)	MSE_tr/val	R^2_val/tr
Basic linear	0.01	0.648	0.02	0.476	0.05	-0.088	0.657	0.734
Ridge	0.01	0.604	0.02	0.539	0.02	0.515	0.863	0.893
Lasso	0.01	0.617	0.02	0.574	0.03	0.341	0.894	0.931
LARS	0.01	0.604	0.02	0.570	0.03	0.429	0.920	0.943
ENR	0.01	0.628	0.01	0.586	0.03	0.488	0.893	0.934
KRR	0.02	0.351	0.03	0.115	0.04	0.086	0.807	0.328
BRR	0.01	0.639	0.01	0.589	0.02	0.577	0.872	0.923
ARD	0.01	0.613	0.02	0.567	0.02	0.539	0.892	0.924
Random Forest	0.00	0.922	0.02	0.446	0.02	0.565	0.147	0.484
Ada Boost	0.01	0.749	0.02	0.448	0.03	0.461	0.462	0.598
Gradient Boost	0.00	0.872	0.02	0.398	0.03	0.367	0.227	0.456
XG Boost	0.00	0.956	0.02	0.333	0.02	0.607	0.071	0.348
SVR	0.01	0.628	0.01	0.588	0.02	0.537	0.896	0.937
KNN	0.00	1.000	0.02	0.238	0.02	0.613	0.000	0.238
PLS	0.02	0.545	0.02	0.497	0.03	0.308	0.927	0.912
GPR	0.03	0.208	0.03	0.042	0.04	0.158	0.893	0.201

Fig. S1 Fitting result summary for EBEW (a~d) and E_g (e~h) prediction models.

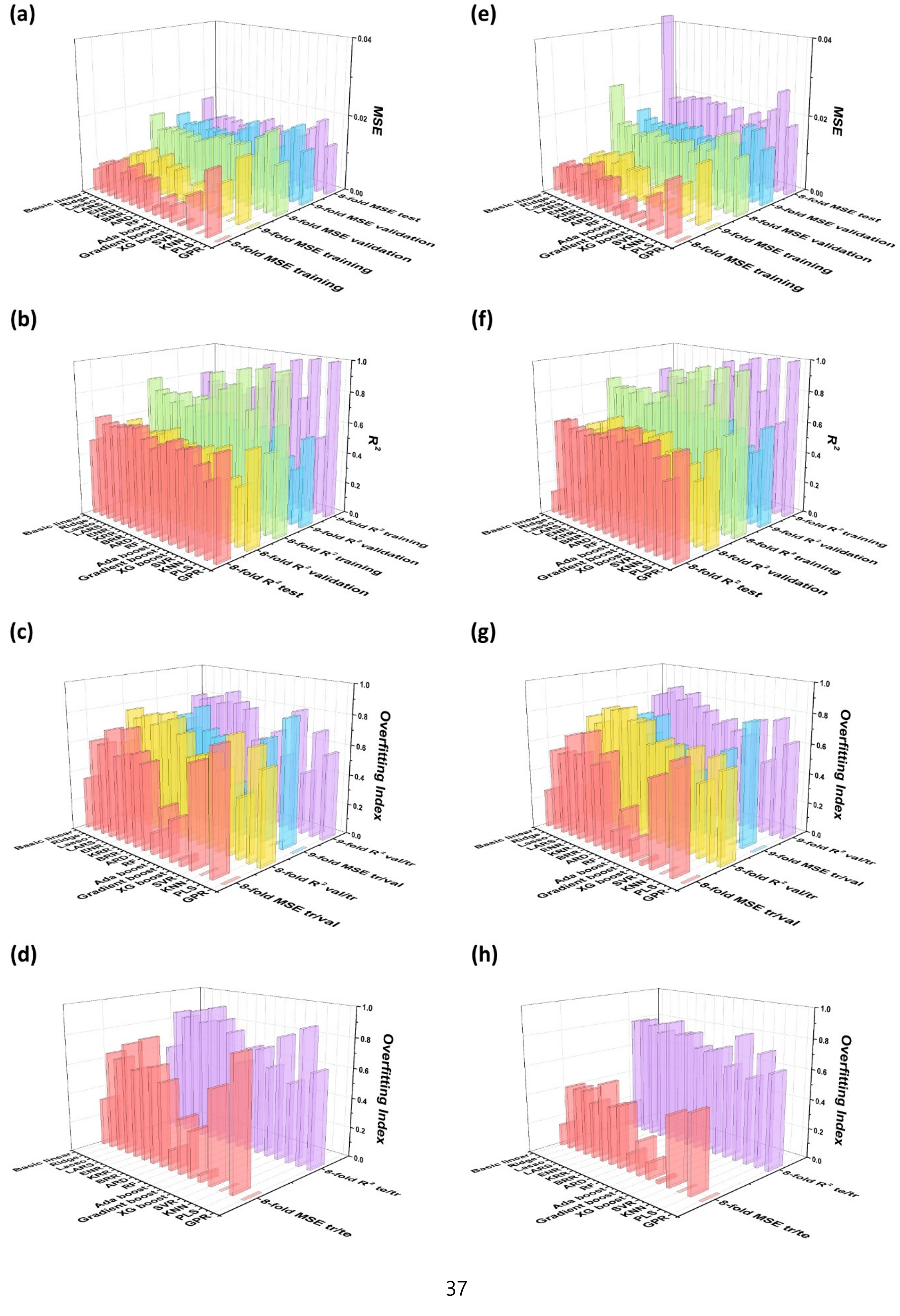

Fig. S2a Plots of predicted vs. experimental PEW for 9-fold cross validation.

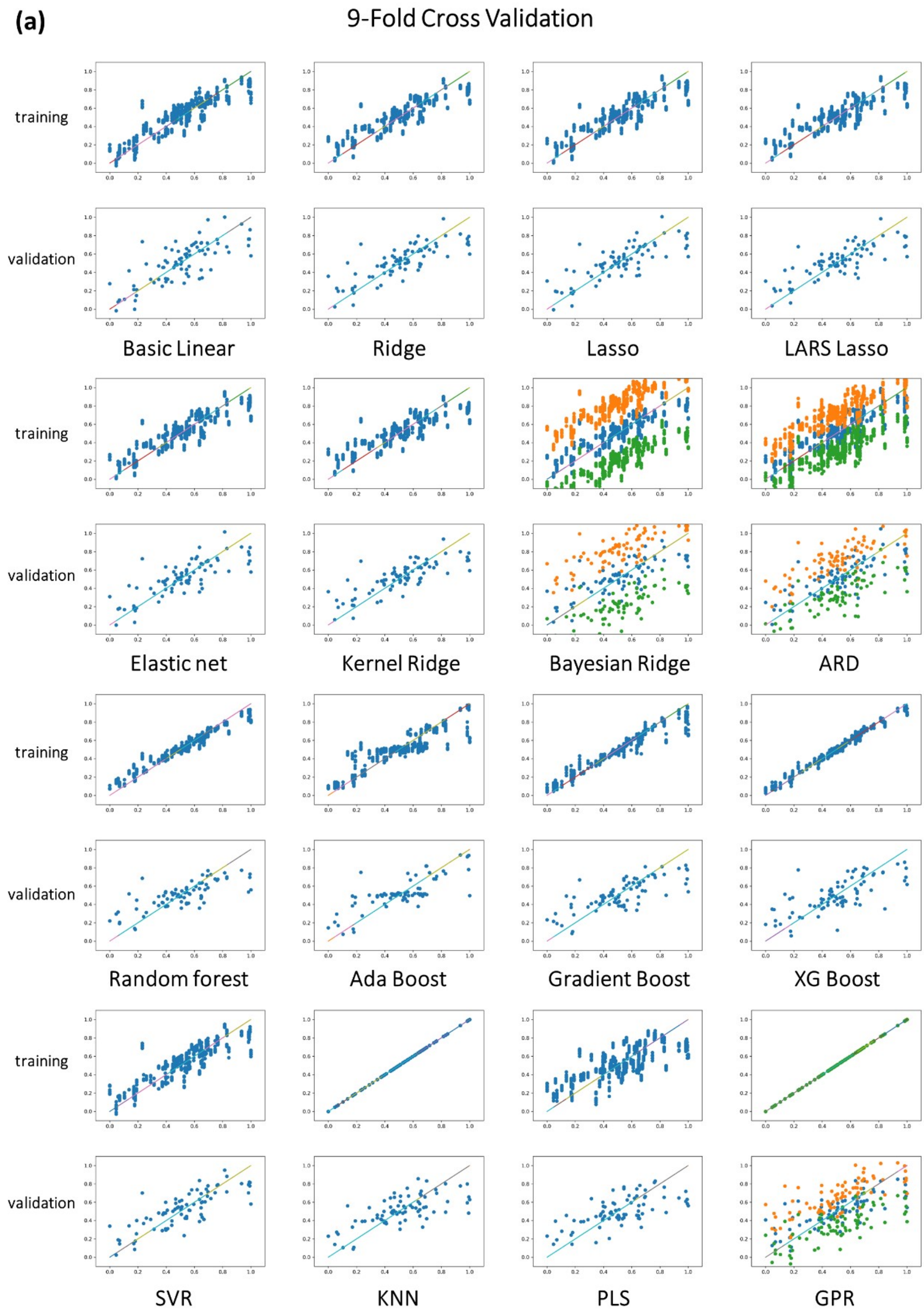

Fig. S2b Plots of predicted vs. experimental EBEW for 9-fold cross validation.

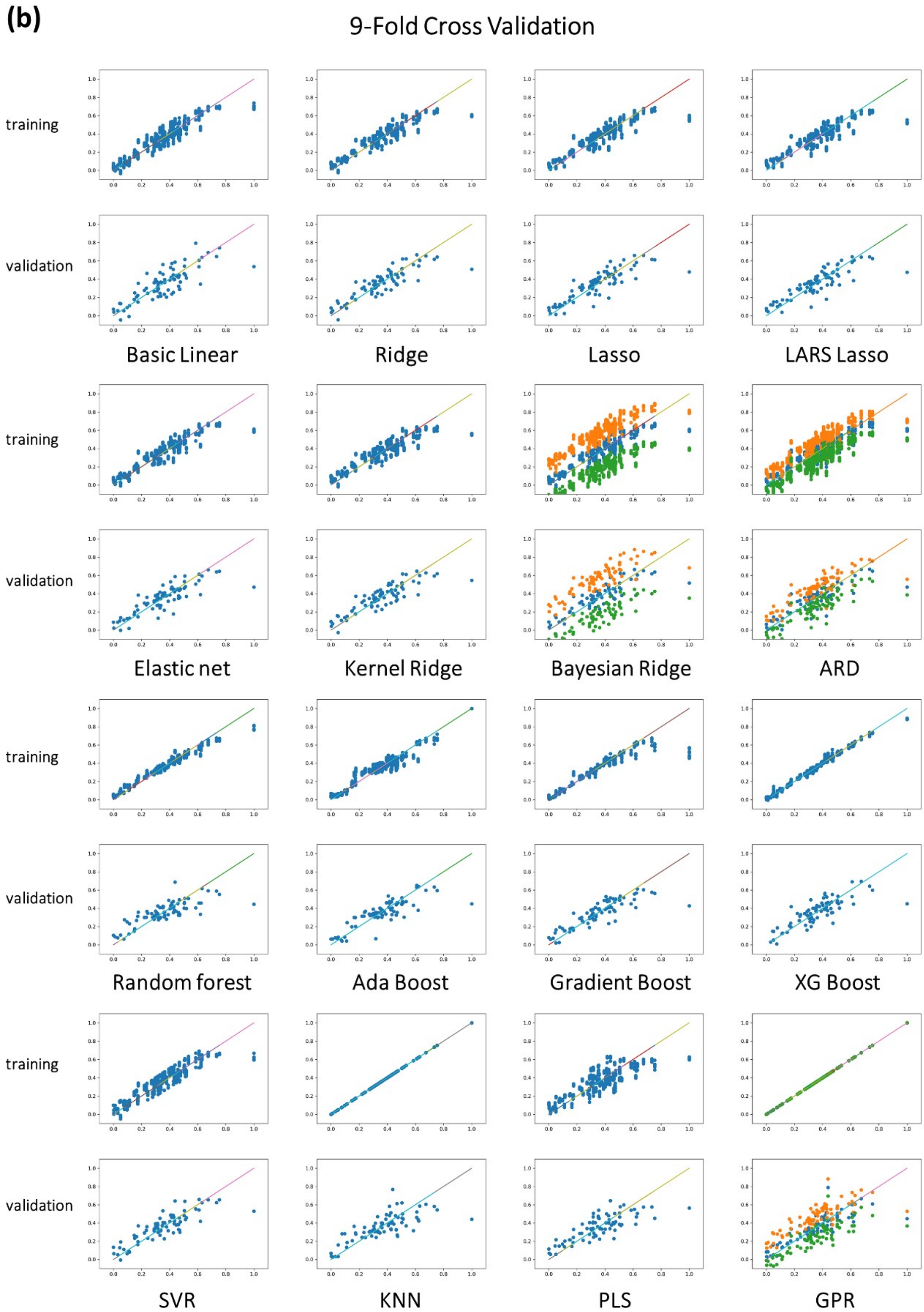

Fig. S2c Plots of predicted vs. experimental E_g for 9-fold cross validation.

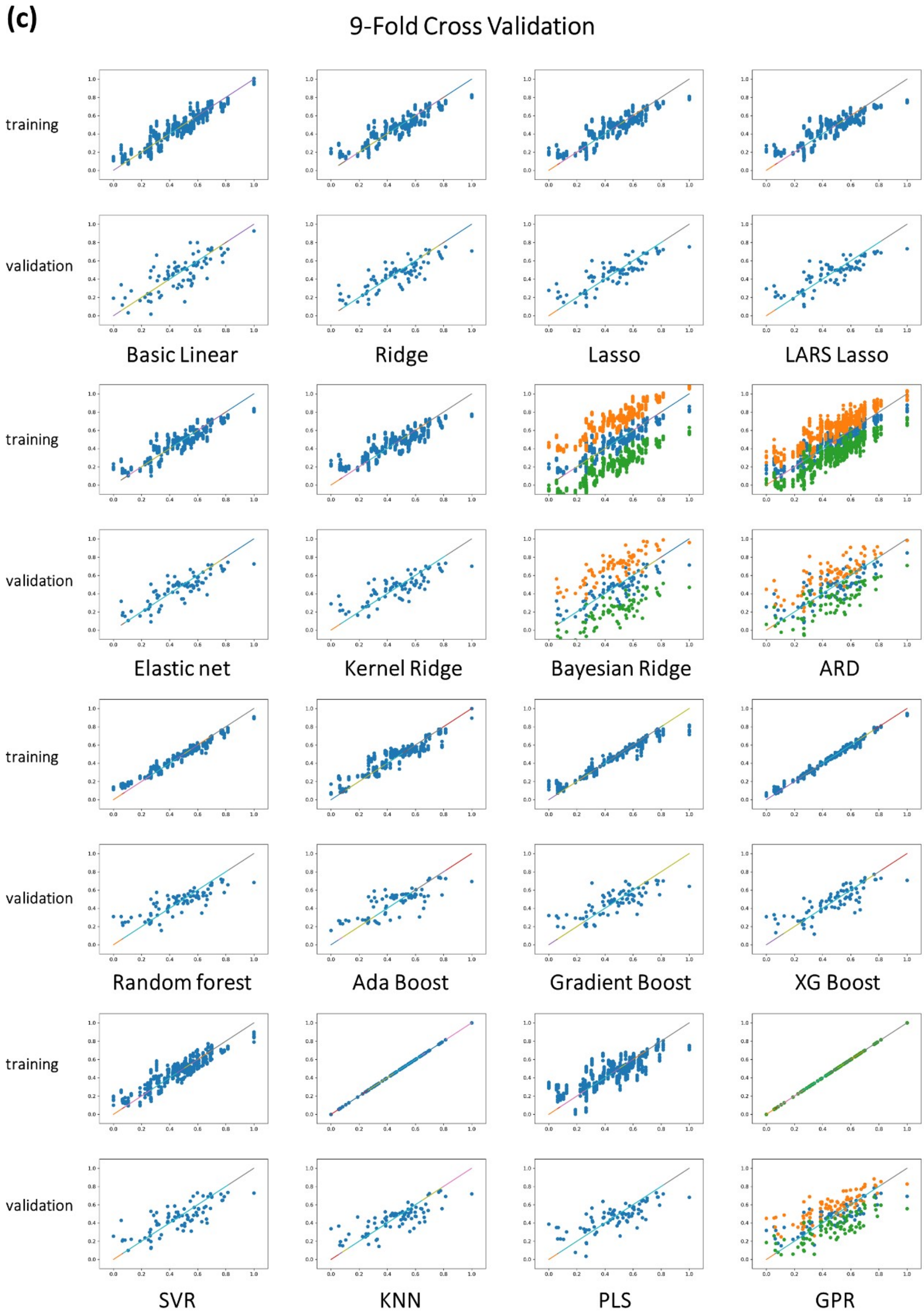

Fig. S3a Plots of ML-predicted vs. experimental PEW for every ML algorithm for leave-one-out cross-validation with no holdout test dataset.

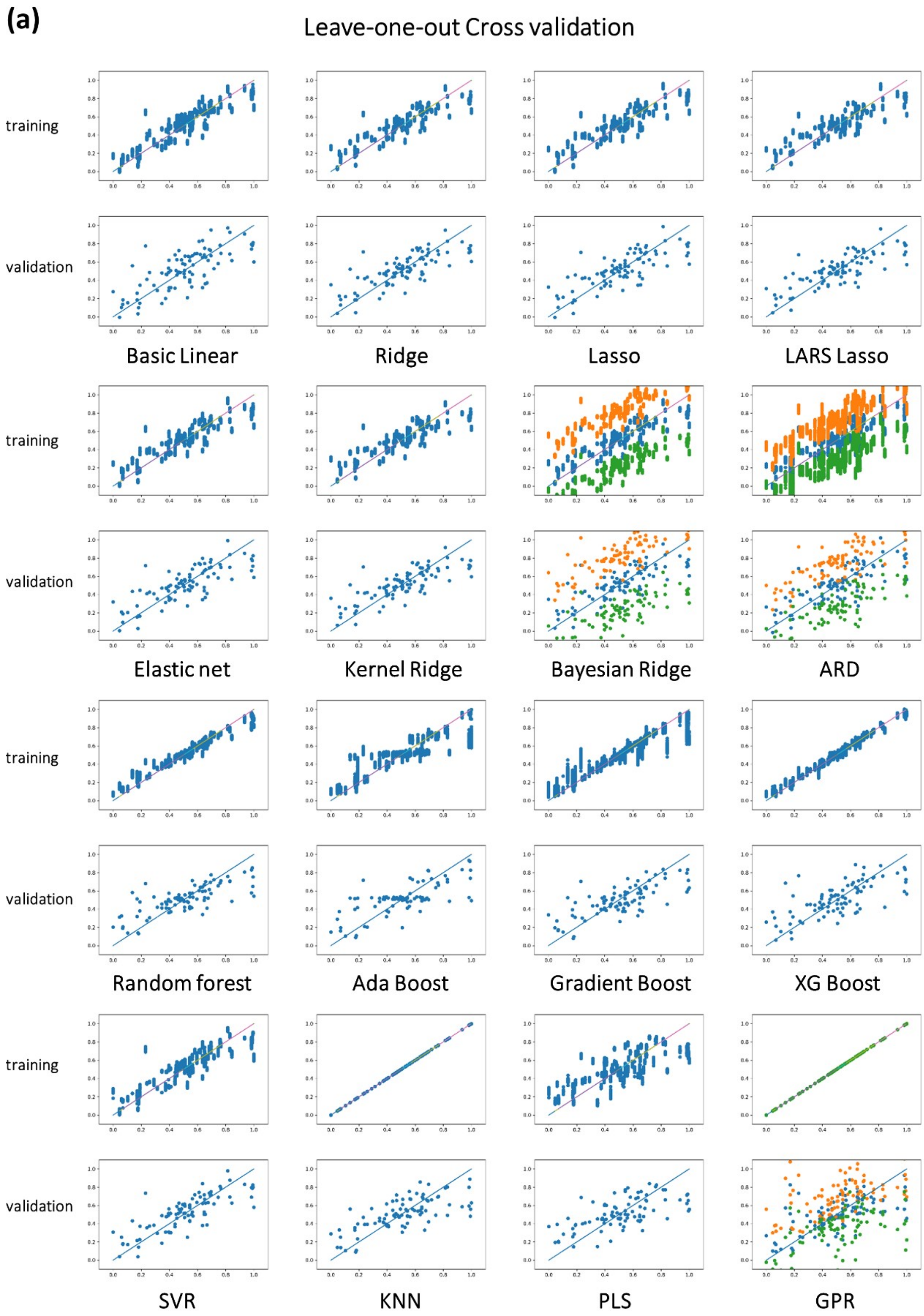

Fig. S3b Plots of ML-predicted vs. experimental EBEW for every ML algorithm for leave-one-out cross-validation with no holdout test dataset.

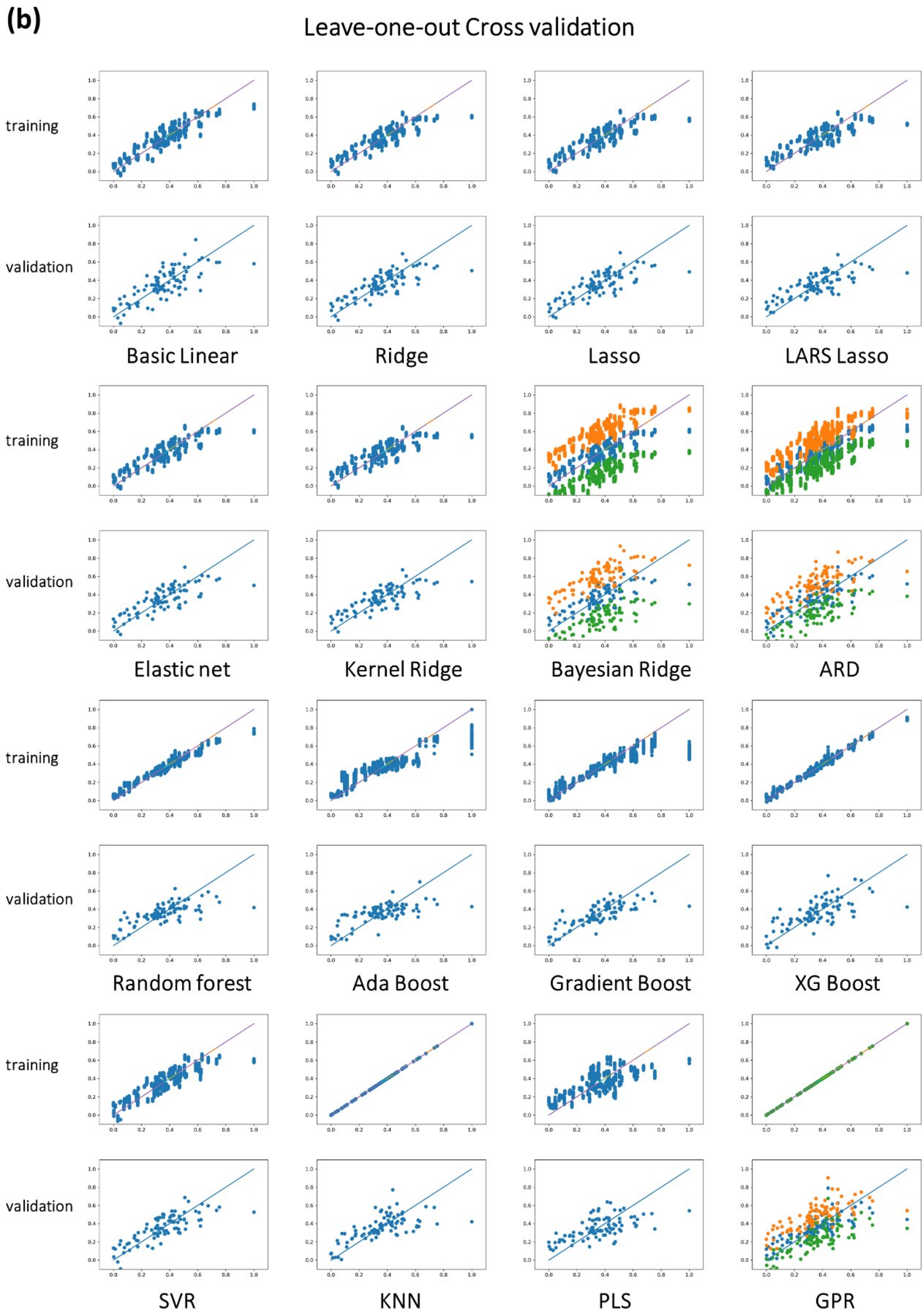

Fig. S3c Plots of ML-predicted vs. experimental E_g for every ML algorithm for leave-one-out cross-validation with no holdout test dataset.

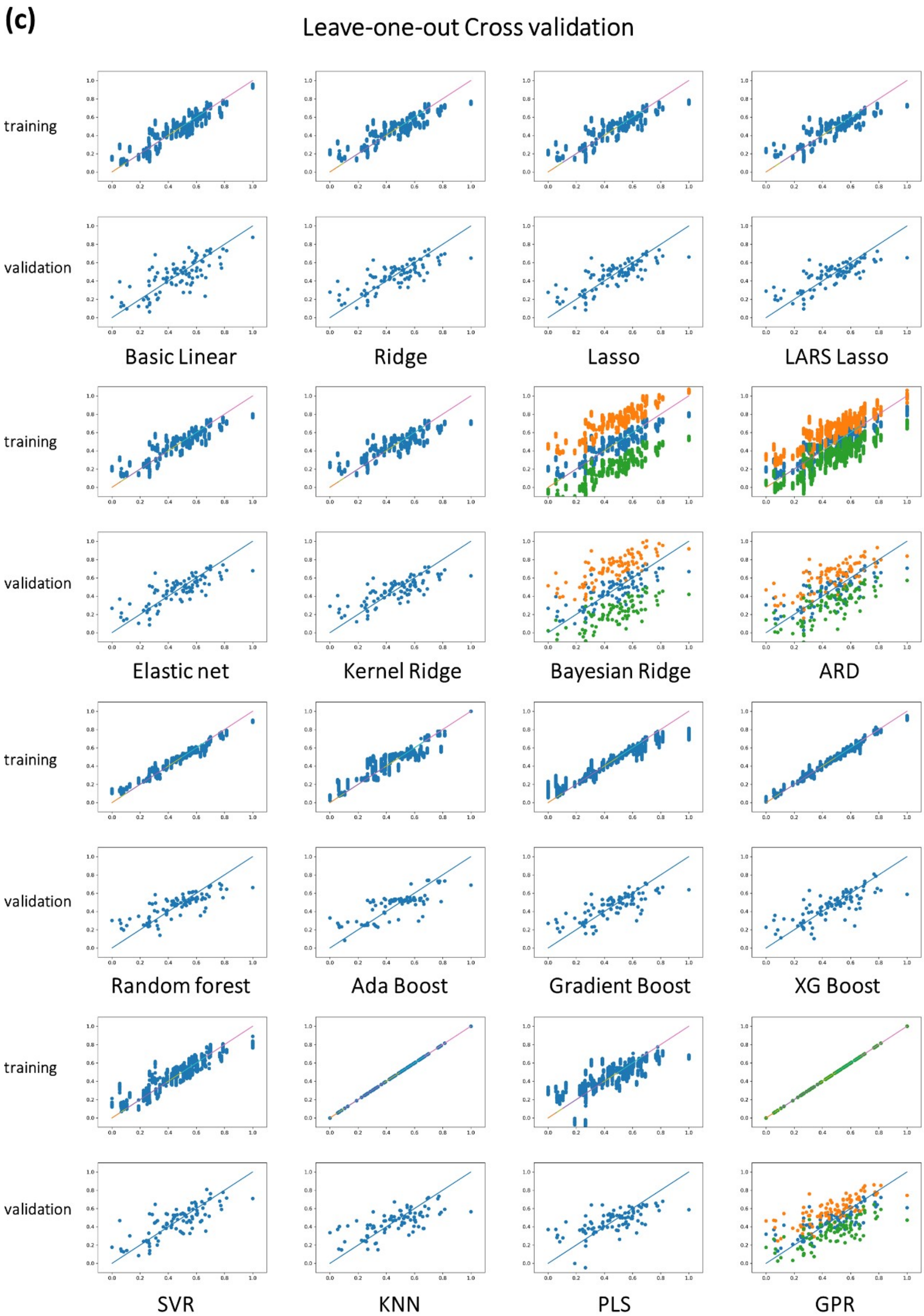

Fig. S4a The surrogate ML model regression results. Plots of the ML-predicted vs. experimental PEW for every ML algorithm for 8-fold cross-validation with a holdout dataset test.

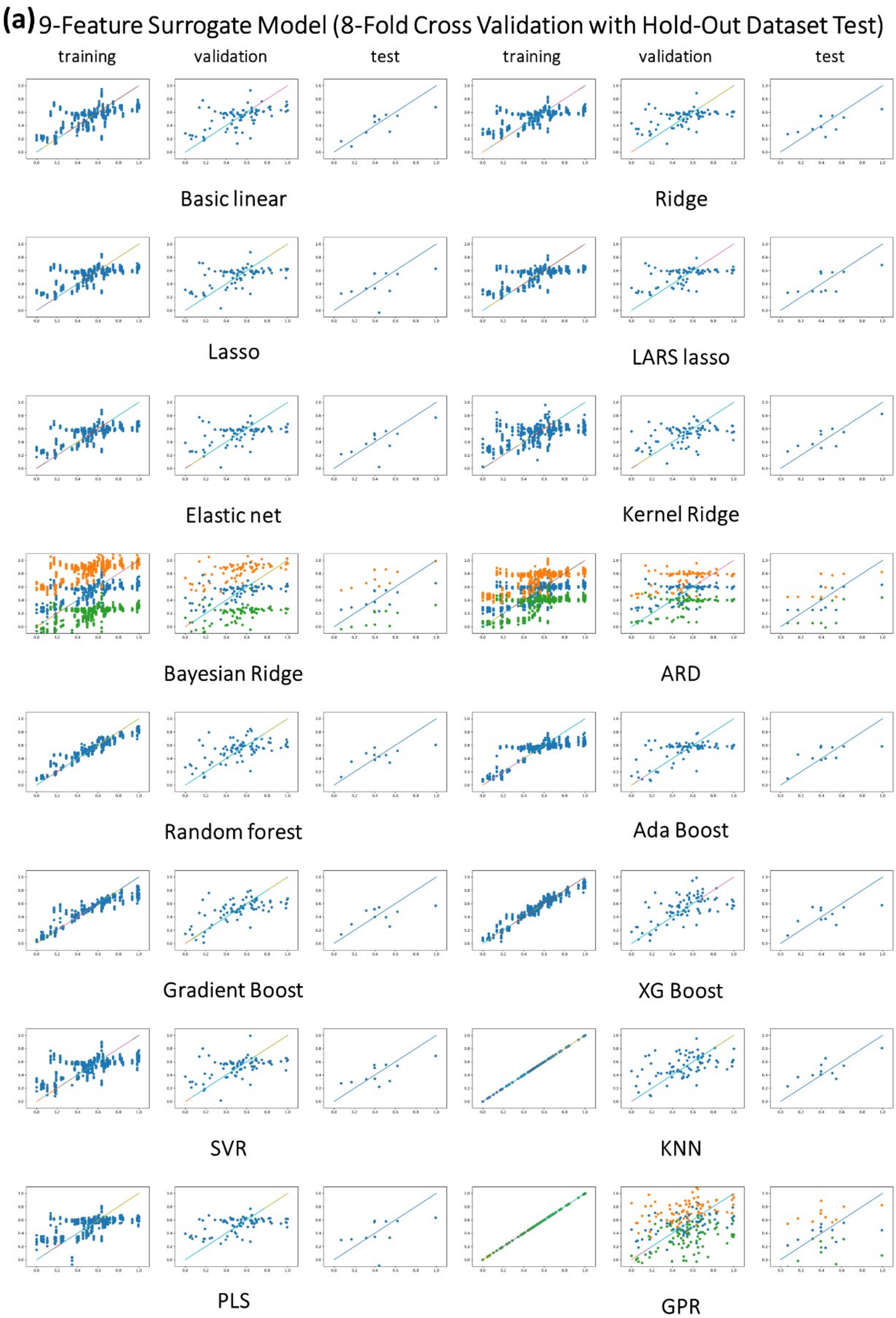

Fig. S4b The surrogate ML model regression results. Plots of the ML-predicted vs. experimental EBEW for every ML algorithm for 8-fold cross-validation with a holdout dataset test.

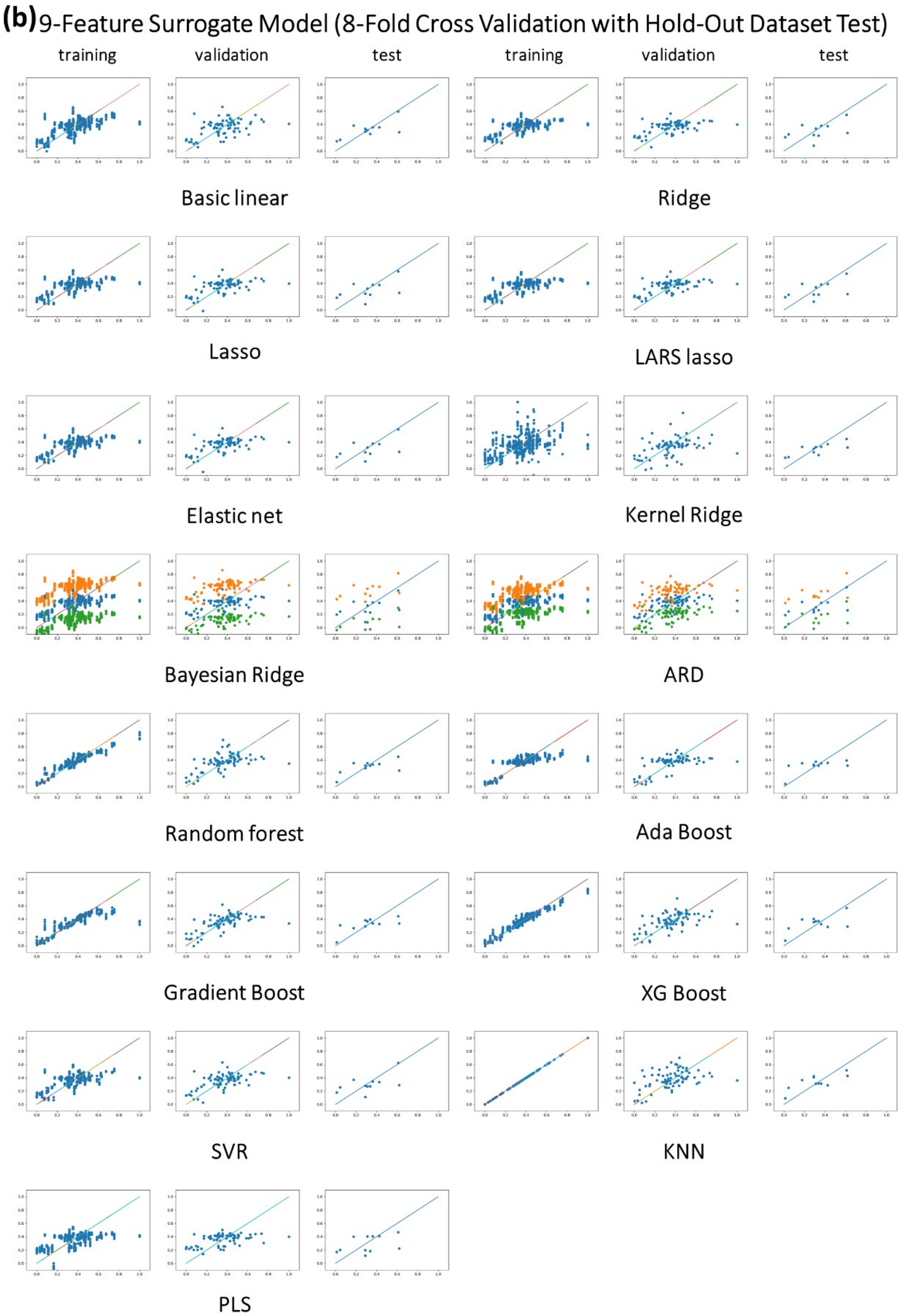

Fig. S4c The surrogate ML model regression results. Plots of the ML-predicted vs. experimental E_g for every ML algorithm for 8-fold cross-validation with a holdout dataset test.

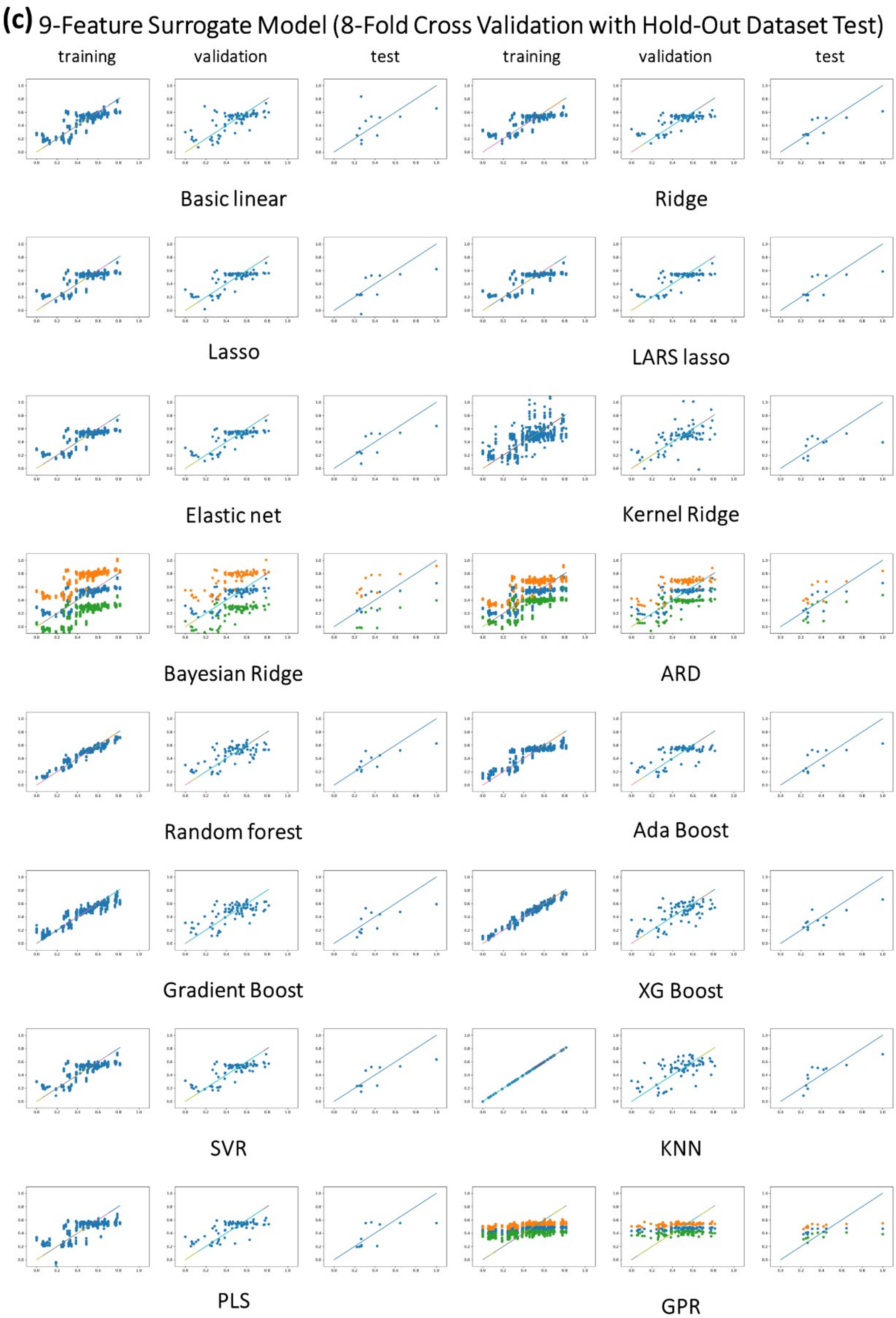

The data sources for the 91 phosphors used for the present investigation.

(The primary number coincides the entry number used in Fig. 2 and Table S3, and -1 and -2 designate multiple sources for a single entry)

(1-1) Z. Tao, Y. Cheng, Y. Huang, P. Cai, H. J. Seo, Luminescence performance and structural characteristic of Eu^{2+}-Activated Na2BaSi2O6 phosphor, *ECS J. Solid State Sci. Technol.*, 2014, **3,** R71-R78.

(1-2) R. P. Gunawardane, M. E. Cradwick, L. S. Dent Glasser, Crystal structure of $Na_2BaSi_2O_6$, *J. Chem. Soc., Dalton Trans.*, 1973, 2397-2400.

(2-1) Y. Q. Li, A. C. A. Delsing, R. Metslaar, G. de With, H. T. Hintzen, Photoluminescence properties of rare-earth activated $BaSi_7N_{10}$, *J. Alloys compd.*, 2009, **487,** 28-33.

(2-2) H. Huppertz, W. Schnick, Edge-sharing SiN_4, tetrahedra in the highly condensed nitridosilicate $BaSi_7N_{10}$, *Chem. Eur. J.*, 1997, **3,** 249-252.

(3-1, 30-1) C. J. Duan, X. J. Wang, W. M. A. Otten, C. A. Delsing, J. T. Zhao, H. T. Hintzen, Preparation, electronic structure, and photoluminescence properties of Eu^{2+}- and Ce^{3+}/Li^{+}-activated alkaline earth silicon nitride $MSiN_2$ (M = Sr, Ba), *Chem. Mater.*, 2008, **20,** 1597-1605.

(3-2, 30-2) Z. A. Gál, P. M. Mallinson, H. J. Orchard, S. J. Clarke, Synthesis and structure of alkaline earth silicon nitrides: $BaSiN_2$, $SrSiN_2$, and $CaSiN_2$, *Inorg. Chem.*, 2004, **43,** 3998-4006.

(4-1) Y. Xu, Z. Song, Z. Yin, D. Zhou, R. Wang, C. Li, J. Qiu, A novel blue-emitting phosphor $MgAl(PO_4)O$: Eu^{2+} for white LEDs, *Adv. Mat. Res.*, 2011, 311-313, 1222-1226.

(4-2) P. Schmid-Beurmann, F. Brunet, V. Kahlenberg, E. Dachs, Polymorphism and thermochemistry of $MgAlPO_4O$, a product of lazulite breakdown at high temperature, *Eur. J. Mineral.*, 2007, **19,** 159-172.

(5) J.-L. Yuan, X.-Y. Zeng, J.-T. Zhao, Z.-J. Zhang, H.-H. Chen, G.-B. Zhang, Rietveld refinement and photoluminescent properties of a new blue-emitting material: Eu^{2+} activated $SrZnP_2O_7$, *J. Solid State Chem*, 2007, **180,** 3310-3316.

(6, 53) J. Brgoch, S. D. Klob, K. A. Denault, R. Seshadri, Accessing $(Ba_{1-x}Sr_x)Al_2Si_2O_8$:Eu phosphors for solid state white lighting via microwave-assisted preparation: tuning emission color by coordination environment, *Z. Anorg. Allg. Chem.*, 2014, **640,** 1182-1189.

(7) F.-C. Lu, L.-J. Bai, B.-Z. Yang, Z.-P. Yang, Synthesis, structure and photoluminescence of $BaAl_2Si_2O_8:Eu^{2+}$ blue-emitting phosphors, *ECS J. Solid State Sci. Technol.*, 2013, **2,** R254-R257.

(8-1) P. F. Smet, N. Avci, K. V. den Eeckhout, D. poelman, Extending the afterglow in $CaAl_2O_4$:Eu,Nd persistent phosphors by electron beam annealing, *Opt. Mater. Express.*, 2012, **2,** 1306-1313.

(8-2) V. I. Ponomarev, D. M. Kheiker, N. V. Belov, Crystal structure of calcium dialuminate, CA2, *Kristallografiya.* 1970, **15,** 1140-1143.

(9-1) S. Yao, L. Xue, Y. Yan, Photoluminescence properties of $M_2ZnSi_2O_7$: Eu^{2+} (M=Sr, Ba), *J. Rare Earths.*, 2010, **28,** 265-268.

(9-2) J. W. Kaiser, W. Jeitschko, Crystal structure of the new barium zinc silicate $Ba_2ZnSi_2O_7$, *Z. Kristallogr. NCS.*, 2002, **217,** 25-26.

(10) Y.-I. Kim, S.-H. Nahm, W. B. Im, D. Y. Jeon, D. H. Gregory, Structural refinement of Eu doped $CaMgSi_2O_6$ using X-ray powder diffraction data, *J. Lumin.*, 2005, **115,** 1-6.

(11) C.-H. Park, Y.-N. Choi, Crystalstructure of $BaMg_2Si_2O_7$ and Eu^{2+} luminescence, *J. Solid State Chem.*, 2009, **182,** 1884-1888.

(12-1) X. Zhang, J. Zhang, R. Wang, M. Gong, Photo-physical behaviors of efficient green phosphor $Ba_2MgSi_2O_7:Eu^{2+}$ and its application in light-emitting diodes, *J. Am. Ceram. Soc.*, 2010, **93,** 1368-1371.

(12-2) M. Ardit, M. Dondi, M. Merlini, G. Cruriani, Melilite-type and melilite-related compounds: structural variations along the join $Sr_{2-2x}Ba_xMgSi_2O_7$ ($0 \le X \le 2$) and high-pressure behavior of the two end-members, *Phys. Chem. Miner.*, 2012, **39,** 199-211.

(13-1, 14-1) W. Y. Huang, F. Yoshimura, K. Ueda, Y. Shimomura, H.-S. Sheu, T.-S. Chan, C.-Y. Chiang, W. Zhou, R.-S. Liu, Chemical pressure control for photoluminescence of $MSiAl_2O_3N_2:Ce^{3+}/Eu^{2+}$ (M = Sr, Ba) oxynitride phosphors, *Chem. Mater.*, 2014, **26,** 2075-2085.

(13-2, 14-2) R. Lauterbach, W. Schnick, Synthese, kristallstruktur und eigenschaften eines neuen sialons-$SrSiAl_2O_3N_2$, *Z. anorg. allg. Chem.*, 1998, **624,** 1154-1158.

(15-1) C. Kulshreshtha, A. K. Sharma, K.-S. Sohn, Effect of Local structures on the luminescence of Li_2 (Sr,Ca,Ba)SiO_4 :Eu^{2+}, *J. Electrochem. Soc.*, 2009, **156,** J52-J56.

(15-2) J. Kim, D. Ahn, C. Kulshreshtha, K.-S. Sohn, N. Shin, Lithium barium silicate, Li_2BaSiO_4, from synchrotron powder data, *Acta Crystallogr. Sect. C: Cryst. Struct. Commun.*, 2009, **65,** i14-i16.

(16-1) Y. Y. Ma, F. Xiao, S. Ye, Q. Y. Zhang, Z. H. Jiang, Y. Qian, Electronic and Luminescence Properties of LiSiON: Eu^{2+}, Eu^{2+}/Mn^{2+} as a Potential Phosphor for UV-Based White LEDs, *ECS J. Solid State Sci. Technol.*, 2012, **1,** R1-R6.

(16-2) Y. Laurent, J. Guyader, G. Roult, Etude par diffraction de neutrons selon la méthode du temps de vol de LiSiONα, *Acta Cryst.*, 1981, **B37,** 911-913.

(17) X. Piao, K.-I. Machida, T. Horikawa, H. Hanzawa, Y. Shimomura, N. Kijima, Preparation of $CaAlSiN_3$:Eu2+ phosphors by the self-propagating high-temperature synthesis and their luminescent properties, *Chem. Mater.*, 2007, **19,** 4592-4599.

(18-1) S.-S. Yao, L.-H. Xue, Y.-W. Yan, Synthesis and luminescent properties of Eu^{2+} doped $BaZn_2Si_2O_7$ phosphors by combustion-assisted synthesis method, *J. Alloys Compd.*, 2011, **509,** 1870-1873.

(18-2) J. H. Lin, G. X. Lu, M. Z. Su, C.-K. Loong, J. W. Richardson Jr, Phase transition and crystal structures of $BaZn_2Si_2O_7$, *J. Phys. Chem. Solids.*, 1999, **60,** 975-983.

(19) W. B. Park, S. P. Singh, K.-S. Sohn, Discovery of a phosphor for light emitting diode applications and its structure determination, $Ba(Si,Al)_5(O,N)_8:Eu^{2+}$, *J. Am. Chem. Soc.*, 2014, **136,** 2363-2373.

(20) H. Watanabe, H. Yamane, N. Kijima, Crystal structure and luminescence of $Sr_{0.99}Eu_{0.01}AlSiN_3$, *J. Solid State Chem.*, 2008, **181,** 1848-1852.

(21) B. Y. Han, S. P. Singh, K.-S. Sohn, Photoluminescent and structural properties of $MgAlSiN_3:Eu^{2+}$ Phosphors, *J. Electrochem. Soc.*, 2011, **158,** J32-J35.

(22) H. Yamane, S. Shimooka, K. Uheda, Synthesis, crystal structure and photoluminescence of a new Eu-doped Sr containing sialon $(Sr_{0.94}Eu_{0.06})(Al_{0.3}Si_{0.7})_4(N_{0.8}O_{0.2})_6$, *J. Solid State Chem.*, 2012, **190,** 264-270.

(23) R.-J. Xie, N. Hirosaki, Y. Li, T. Takeda, Photoluminescence of $(Ba_{1-x}Eu_x)Si_6N_8O$ ($0.005 \le x \le 0.2$) phosphors, *J. Lumin.*, 2010, **130,** 266-269.

(24-1) K. Shioi, N. Hirosaki, R.-J. Xie, T. Takeda, Y. Li, Luminescence properties of $SrSi_6N_8:Eu^{2+}$, *J. Mater. Sci.*, 2008, **43,** 5659-5661.

(24-2) F. Stadler, O. Oeckler, J. Senker, H. A. Höppe, P. Kroll, W. Schnick, $SrSi_6N_8$-A reduced nitridosilicate with a Si-Si bond, *Angew. Chem. Int. Ed.*, 2005, **44,** 567-570.

(25-1) C. J. Duan, W. M. Otten, A. C. A. Delsing, H. T. Hintzen, Photoluminescence properties of Eu^{2+}-activated sialon s-phase $BaAlSiO_2N_7$, *J. Alloys Compd.*, 2008, **461,** 454-458.

(25-2) S. Esmaeilzadeh, J. Grins, Z. Shen, M. Edén, M. Thiaux, Study of sialon s-phases $M_2Al_xSi_{12-x}N_{16-x}O_{2+x}$, M = Ba and $Ba_{0.9}Eu_{0.1}$, by X-ray single crystal diffraction, X-ray powder diffraction, and solid-state nuclear magnetic resonance, *Chem. Mater.*, 2004, **16,** 2113-2120.

(26-1) X. Lan, Q. Wei, Y. Chen, W. Tang, Luminescence properties of Eu^{2+}-activated $KMg_4(PO_4)_3$ for blue-emitting phosphor, *Opt. Mater.*, 2012, **34,** 1330-1332.

(26-2) P. E. Tomaszewski, M. Maczka, A. Majchrowski, A. Waskowska, J. Hanuza, Crystal structure and vibrational properties of $KMg_4(PO_4)_3$, *Solid State Sci.*, 2005, **7,** 1201-1208.

(27-1) V. Bachmann, C. Ronda, O. Oeckler, W. Schnick, A. Meijerink, Color Point Tuning for $(Sr,Ca,Ba)Si_2O_2N_2:Eu^{2+}$ for White Light LEDs, *Chem. Mater.*, 2009, **21,** 316-325.

(27-2) J. A. Kechele, O. Oeckler, F. Stadler, W. Schnick, Structure elucidation of $BaSi_2O_2N_2$ – A host lattice for rare-earth doped luminescent materials in phosphor-converted (pc)-LEDs, *Solid State Sci.*, 2009, **11,** 537–543.

(28-1, 35-1) P. P. Pal, P. K. Baitha, N. Borgohain, J. Manam, Enhanced photoluminescence emission from $XSO_4:Eu^{2+}$ (X = Mg, Sr) microphosphors, *Indian J. Phys.*, 2014, **88,** 243-250.

(28-2) J. Coing-Boyat, Structure de la forme hautes temperatures du sulfate anhydre de magnesium, beta-$MgSO_4$, *Acad. Sci. Comptes Rendus.*, 1962, **255,** 1962-1964.

(29-1) S. T. Taide, N. B. Ingle, S. K. Omanwar, Optimization and improvement in photoluminescence of rare earth activated willemite salt ($CaSO_4$: Eu^{2+}) prepared by co-precipitation method, *IOSR J. Appl. Phys.*, 2014, 4-6.

(29-2) H. Morikawa, T. Tomita, I. Minato, S. I. Iwai, Anhydrite: a refinement, *Acta Cryst.*, 1975, **B31**, 2164-2165.

(31-1) H. J. Song, D. K. Yim, H.-S. Roh, I. S. Cho, S.-J. Kim, Y.-H. Jin, H.-W. Shim, D.-W. Kim, K. S. Hong, $RbBaPO_4:Eu^{2+}$: a new alternative blue-emitting phosphor for UV-based white lightemitting diodes, *J. Mater. Chem. C.*, 2013, **1,** 500-505.

(31-2) L. ElAmmari, B. Elouadi, Crystal structure of the orthophosphate $RbBaPO_4$, *J. Alloys Compd.*, 1992, **188,** 99-101.

(32-1) J. Manam, P. Kumari, S. Das, Characterization and photoluminescence studies of Eu^{2+}-doped $BaSO_4$ phosphor prepared by the recrystallization method, *Appl Phys A.*, 2011, **104,** 197-203.

(32-2) R. W. James, W. A. Wood, The crystal structures of barites, celestine and anglesite, *Proc. Math.*

Phys. Eng. Sci., 1925, **109,** 598-620.

(33, 34) M. P. Saradhi, S. Boudin, U. V. Varadaraju, B. Raveau, A new $BaB_2Si_2O_8$:Eu^{2+}/Eu^{3+}, Tb^{3+} phosphor –synthesis and photoluminescence properties, *J. Solid State Chem.*, 2010, **183,** 2496-2500.

(35-2) K. Burger, D. Cox, R. Papoular, W. Prandl, The application of resonant scattering techniques to Ab initio structure solution from powder data using $SrSO_4$ as a test case, *J. Appl. Cryst.*, 1998, **31,** 789-797.

(36) P. Pust, F. Hintze, C. Hecht, V. Weiler, A. Locher, D. Zitnanska, S. Harm, D. U. Wiechert, P. J. Schmidt; W. Schnick, Group (III) nitrides $M[Mg_2Al_2N_4]$ (M = Ca,Sr,Ba,Eu) and $Ba[Mg_2Ga_2N_4]$ structural relation and non-typical luminescence properties of Eu^{2+} doped samples, *Chem. Mater.*, 2014, **26,** 6113-6119.

(37-1) C. Liu, S. Zhang, Z. Liu, H. Liang, S. Sun, Y. Tao, A potential cyan-emitting phosphor $Sr_8(Si_4O_{12})Cl_8$:Eu^{2+} for wide color gamut 3D-PDP and 3D-FED, *J. Mater. Chem. C.*, 2013, **1,** 1305-1308.

(37-2) J. Wang, G. Li, S. Tian, F. Liao, X. Jing, The composition, luminescence, and structure of Sr_8 $[Si_4O_{12}]Cl_8$:Eu^{2+}, *Mater. Res. Bull.*, 2001, **36,** 2051-2057.

(38) P. Pust, A. S. Wochnik, E. Baumann, P. J. Schmidt, D. Wiechert, C. Scheu, W. Schnick, $Ca[LiAl_3N_4]$:Eu^{2+} A narrow-band red-emitting nitridolithoaluminate, *Chem. Mater.*, 2014, **26,** 3544-3549.

(39) S. Schmiechen, H. Schneider, P. Wagatha, C. Hecht, P. J. Schmidt, W. Schnick, Toward new phosphors for application in illumination-grade white pc-LEDs: the nitridomagnesosilicates $Ca[Mg_3SiN_4]$:Ce^{3+}, $Sr[Mg_3SiN_4]$:Eu^{2+}, and $Eu[Mg_3SiN_4]$, *Chem. Mater.*, 2014, **26,** 2712-2719.

(40-1) R. P. Sonekar, S. K. Omanwar, S. V. Moharil, Combustion synthesis and photoluminescence of Eu^{2+} doped BaB_8O_{13}, *Indian J. Pure & Appl. Phys.*, 2009, **47,** 441-443.

(40-2) J. Krogh-Moe, M. Ihara, On the crystal structure of barium tetraborate, $Ba_{0.4}B_2O_3$, *Acta Cryst.*, 1969, **B25,** 2153-2154.

(41) Y. Luo, Z. G. Xia, Effect of partial nitridation on the structure and luminescence properties of melilite-type $Ca_2Al_2SiO_7$:Eu^{2+} phosphor, *Opt. Mater.*, 2014, **36,** 1874-1878.

(42) C.-H. Huang, Y.-T. Lai, T.-S. Chan, Y.-T. Yeh, W.-R. Liu, A novel green-emitting $SrCaSiAl_2O_7$:Eu^{2+} phosphor for white LEDs, *RSC Adv.*, 2014, **4,** 7811-7817.

(43) Y. Q. Li, N. Hirosaki, R.-J. Xie, M. Mitomo, Crystal, electronic and luminescence properties of

Eu^{2+}-doped $Sr_2Al_{2-x}Si_{1+x}O_{7-x}N_x$, *Sci. Technol. Adv. Mater.*, 2007, **8,** 607-616.

(44-1) L. Jiang, C. Chang, D. Mao, B. A Zhang, new long persistent blue-emitting $Sr_2ZnSi_2O_7$:Eu^{2+}, Dy^{3+} prepared by sol-gel method, *Mater. Lett.*, 2004, **58,** 1825-1829.

(44-2) M. Ardit, G. Cruciani, M. Dondi, The crystal structure of Sr-hardystonite, $Sr_2ZnSi_2O_7$, *Z. Kristallogr.*, 2010, **225,** 298-301.

(45) L. Jiang, C. Chang, D. Mao, C. Feng, Concentration quenching of Eu^{2+} in $Ca_2MgSi_2O_7$:Eu^{2+} phosphor, *Mater. Sci. Eng.*, 2003, **B103,** 271-275.

(46-1) K. H. Kwon, W. B. Im, D. Y. Jeon, Energy transfer in $Sr_2MgSi_2O_7$:Eu^{2+} phosphors in nano scale and their application to solid state lighting with excellent color rendering, *J. Nanosci. Nanotechnol.*, 2013, **13,** 4079-4083.

(46-2) H. Yang, R. M. Hazen, R. T. Downs, L. W. Finger, Structural change associated with the incommensurate-normal phase transition in akermanite, $CaMgSi_2O_7$, at high pressure, *Phys. Chem. Miner.*, 1997, **24,** 510-519.

(47-1) X. Zhang, J. Zhang, J. Xu, Q. Su, Luminescent properties of Eu^{2+}-activated $SrLaGa_3S_6O$ phosphor, *J. alloys. Compd.*, 2005, **389,** 247-251.

(47-2) C. L. Teske, On oxidesulfides of Akermanitetype-structure $CaLaGa_3S_6O$, $SrLaGa_3S_6O$, $La_2ZnGa_2S_6O$, and $Sr_2ZnGe_2S_6O$, *Z. Anorg. Allg. Chem.*, 1950, **531,** 52-60.

(48-1) J. Liu, J. Sun, C. Shi, A new luminescent material: Li_2CaSiO_4:Eu^{2+}, *Mater. Lett.*, 2006, **60,** 2830-2833.

(48-2) J. A. Gard, A. R. West, Preparation and crystal structure of Li_2CaSiO_4 and isostructural Li_2CaGeO_4, *J. Solid State Chem.*, 1973, **7,** 422-427.

(49-1, 50-1) S. Su, W. Liu, R. Duan, L. Cao, G. Su, C. Zhao, Near UV-pumped bluish-white emitting K(Ba,Sr,Ca)BP_2O_8:Eu^{2+} phosphors, *J. alloys compd.*, 2013, **575,** 309-313.

(49-2, 50-2) D. Zhao, W.-D. Cheng, H. Zhang, S.-P. Huang, Z. Xie, W.-L. Zhang, S.-L. Yang, $KMBP_2O_8$ (M = Sr, Ba): A new kind of noncentrosymmetry borophosphate with the three-dimensional diamond-like framework, *Inorg. Chem.*, 2009, **48,** 6623-6629.

(51-1) B. Yuan, Y. Huang, Y. M. Yu, S. I. Kim, H. J. Seo, A new blue-emitting phosphor of Eu^{2+}-doped $BaMgSi_4O_{10}$, *Mater. Lett.*, 2012, **70,** 57-59.

(51-2) R. M. Hazen, L. W. Finger, High-pressure and high-temperature crystallographic study of the gillespite I-II phase transition, *Am. Mineral.*, 1983, **68,** 595-603.

(52) M. Jiao, Y. Jia, W. Lü, W. Lv, Q. Zhao, B. Shao, You, H. $Sr_3GdNa(PO_4)_3F{:}Eu^{2+},Mn^{2+}$: a potential color tunable phosphor for white LEDs, *J. Mater. Chem. C.*, 2014, **2,** 90-97.

(54-1) L. Liu, R.-J. Xie, N. Hirosaki, B. Dierre, T. Sekiguchi, Luminescence properties of a blueemitting phosphor:$(Sr_{1-x}Eu_x)Si_9Al_{19}ON_{31}$ ($0 < x \leq 1$), *J. Solid State Chem.*, 2013, **207,** 49-54.

(54-2) J. Grins, S. Esmaeilzadeh, G. Svensson, Z. J. Shen, High-resolution electron microscopy of a Sr-containing sialon polytypoid phase, *J. Eur. Ceram. Soc.*, 1999, **19,** 2723-2730.

(55-1) M. P. Saradhi, U. V. Varadaraju, Photoluminescence studies on Eu^{2+}-activated Li_2SrSiO_4-a potential orange-yellow phosphor for solid-state lighting, *Chem. Mater.*, 2006, **18,** 5267-5272.

(55-2) Y. Hirano, T. Iwata, K. Momma, K. Fukuda, Electron density distribution and crystal structure of lithium strontium silicate, Li_2SrSiO_4, *Powder Diffr.*, 2010, **25,** 4-8.

(56-1) Y. Lan, L. Yi, L. Zhou, Z. Tong, F. Gong, R. Wang, Synthesis and luminescence properties of $SrBPO_5{:}Eu^{2+}$, Mn^{2+} phosphor for light-emitting diodes, *Physica B.*, 2010, **405,** 3489-3491.

(56-2) S. Pan, W. Xicheng, F. P. Zhen, Z. Guochun, L. Zhihua, D. Chenxia, C. Chuangyan, Growth, structure and properties of single crystals of $SrBPO_5$, *Chem. Mater.*, 2003, **15,** 2218-2221.

(57, 58) K. Shioi, N. Hirosaki, R.-J. Xie, T. Takeda, Y. Q. Li, Y. Matsushita, Synthesis, crystal structure, and photoluminescence of Sr-α-SiAlON:Eu^{2+}, *J. Am. Ceram. Soc.*, 2010, **93,** 465-469.

(59-1) X. Zhang, F. Mo, L. Zhou, M. Gong, Properties–structure relationship research on $LiCaPO_4{:}Eu^{2+}$ as blue phosphor for NUV LED application, *J. Alloys compd.*, 2013, **575,** 314-318.

(59-2) P. Lightfoot, M. C. Pienkowski, P. G. Bruce, I. Abrahams, Synthesis and structure of $LiCaPO_4$, by combined X-ray and neutron powder diffraction, *J. Mater. Chem.*, 1991, **1,** 1061-1063.

(60) Z. Tao, Y. Huang, P. Cai, I. Kim, H. J. Seo, Synthesis and efficient blue-emitting of Eu^{2+}- activated borate fluoride $BaAlBO_3F_2$, *Opt. Mater.*, 2014, **37,** 287-292.

(61-1) R. Yu, H. Li, H. Ma, C. Wang, H. Wang, Luminescence centers and spectrum characteristics of a novel Eu^{2+}-activated hexa-aluminate $CaZrBAl_9O_{18}$, *Phys. Status Solidi. A.*, 2014, **211,** 811-816.

(61-2) T. Armbruster, N. Döbelin, A. Peretti, D. Günther, E. Reusser, B. Grobėty, The crystal structure of painite $CaZrB[Al_9O_{18}]$ recisited, *Am. Mineral.*, 2004, **89,** 610-613.

(62) Y. Q. Li, C. M. Fang, G. de With, H. T. Hintzen, Preparation, structure and photoluminescence properties of Eu^{2+} and Ce^{3+}-doped $SrYSi_4N_7$, *J. Solid state Chem.*, 2004, **177,** 4687-4694.

(63, 64, 65) T. Horikawa, M. Fujitani, H. Hanazawa, K.-I. Machida, Structure and photoluminescence properties of $MIIMIIISi_4N_7:Eu^{2+}$ (MII = Ca, Sr, Ba / MIII = Sc, Y, La) phosphors prepared by carbothermal reduction and nitridation, *ECS J. Solid State Sci. Technol.*, 2012, **1,** R113-R118.

(66) D.-Y. Wang, C.-H. Huang, Y.-C. Wu, T.-M. Chen, $BaZrSi_3O_9:Eu^{2+}$: a cyan-emitting phosphor with high quantum efficiency for white light-emitting diodes, *J. Mater Chem.*, 2011, **21,** 10818-10822.

(67) D. Y. Wang, Y. C. Wu, T. M. Chen, Synthesis, crystal structure, and photoluminescence of a novel blue-green emitting phosphor: $BaHfSi_3O_9:Eu^{2+}$, *J. Mater. Chem.*, 2011, **21,** 18261-18265.

(68-1) J. Chen, Y.-G. Liu, H. Liu, D. Yang, H. Ding, M. Fang, Z. Huang, The luminescence properties of novel α-$Mg_2Al_4Si_5O_{18}:Eu^{2+}$ phosphor prepared in air, *RCS adv.*, 2014, **4,** 18234-18239.

(68-2) P. Predecki, J. Haas, J. Faber, R. L. Hitterman, Structural aspects of the lattice thermal expansion of hexagonal cordierite, *J. Am. Ceram. Soc.*, 1987, **70,** 175-182.

(69-1) T. L. Zhou, Z. Song, X. P. Song, L. Bian, Q. L. Liu, A red oxide phosphor, $Sr_2ScAlO_5:Eu^{2+}$ with perovskite-type structure, for white light-emitting diodes, *Chin. Phys. B.*, 2010, **19,** 127808-1-4.

(69-2) M. Rath, H. Müller-Buschbaum, Ein beitrag zur kristallstruktur von Ba_2ScAlO_5 und $Sr_2Sc_{0.5}Al_{1.5}O_5$, *J. Alloys Compd.*, 1992, **189,** 127-130.

(70-1) T.-W. Kuo, C.-H. Huang, T.-M. Chen, Novel yellowish-orange $Sr_8Al_{12}O_{24}S_2:Eu^{2+}$ phosphor for application in blue light-emitting diode based white LED, *Opt. Express.*, 2010, **18,** A231-A236.

(70-2) M. E. Brenchley, M. T. Weller, Synthesis and structure of sulfide aluminate sodalities, *J. Mater. Chem.*, 1992, **2,** 1003-1005.

(71-1) S.-J. Gao, T. Li, Z.-C. Zhang, P.-L. Li, Z.-J. Wang, Z.-P. Yang, $Sr_3Bi(PO_4)_3$:Eu^{2+} Luminescence, concentration quenching and crystallographic sites, *Chin. Phys. Lett.*, 2014, **31,** 073301-073304.

(71-2) P. P. Sahoo, T. N. G. Row, Crystal chemistry of the noncentrosymmetric eulytites:$A_3Bi(XO_4)_3$ (X = V, A = Pb; X = P, A = Ca, Cd, Sr, Pb), *Inorg. Chem.*, 2010, **49,** 10013-10021.

(72) Z. Jiang, Z. Sun, X. Su, L. Duan and X. Yu, Crystal structure and luminescence properties of Eu^{2+} activated $Sr_{12}Al_{14}O_{32}Cl_2$: A potential green-emitting phosphor for near UV light-emitting diodes, *J. Alloys Compd.*, 2013, **577,** 683-686.

(73) T. Iwata, M. Haniuda and K. Fukuda, Crystal structure of $Ca_{12}Al_{14}O_{32}Cl_2$ and luminescence properties of $Ca_{12}Al_{14}O_{32}Cl_2:Eu^{2+}$, *J. Solid State Chem.*, 2008, **181,** 51-55.

(74-1) W. Zhang, D. Wie and H. J. Seo, Eu^{2+}-doped pollucite $CsAlSi_2O_6$ with high luminescence efficiency for UV-pumped light-emitting diodes, *Mater. Lett.*, 2013, **94,** 140-142.

(74-2) S. Naray-Szabo, Die struktur des pollucits $CsAlSi_2O_6 \cdot H2O$, *Zeitschrift für Kristallographie*, 1938, **99,** 277–282.

(75) Q. Wang, D. Deng, S. Xu, Y. Hua, L. Huang, H. Wang, S. Zhao, G. Jia and C. Li, Crystal structure and photoluminescence properties of Eu^{2+}-activated $Ba_2LiB_5O_{10}$ phosphors, *Opt. Commun.*, 2011, **284,** 5315-5318.

(76) R.S. Palaspagar, A.B. Gawandea, R.P. Sonekar and S.K. Omanwar, $Eu^{3+} \rightarrow Eu^{2+}$ reduction in $BaAl_2B_2O_7$ phosphor in oxidizing environment, *Optik*, 2015, **126,** 5030-5032.

(77) K.-Y. Yeh, C.-C. Yang, W.-R. Liu and M.G. Brik, Novel blue-emitting phosphors - $BaBeSiO_4:Eu^{2+}$: luminescence properties and its application for UV-light emitting diodes, *Opt Mater Express*, 2016, **6,** 416-428.

(78) S.-P. Lee, T.-S. Chan, S. Dutta and T.-M. Chen, Novel Eu^{2+}-activated thiogallate phosphors for white LED applications: structural and spectroscopic analysis, *RSC Adv.*, 2018, **8,** 11725-11730.

(79) S. Schmiechen, P. Strobel, C. Hecht, T. Reith, M. Siegert, P. J. Schmidt, P. Huppertz, D. Wiechert and W. Schnick, Nitridomagnesosilicate $Ba[Mg_3SiN_4]:Eu^{2+}$ and Structure–Property Relations of Similar Narrow-Band Red Nitride Phosphors, *Chem. Mater.*, 2015, **27,** 1780-1785.

(80) Y.-K. Kim, S. Choi and H.-K. Jung, Photoluminescence properties of Eu^{2+} and Mn^{2+}-activated $BaMgP_2O_7$ as a potential red phosphor for white-emission, *J. Lumin.*, 2010, **130,** 60-64.

(81) C. Zhao, Z. Xia and M. Li, Eu^{2+}-activated full color orthophosphate phosphors for warm white light-emitting diodes, *RSC Adv.*, 2014, **4,** 33114.

(82) Z. C. Wu, J. X. Shi, J. Wang, M. L. Gong and Q. Su, A novel blue-emitting phosphor $LiSrPO_4:Eu^{2+}$ for white LEDs, *J. Solid State Chem.*, 2006, **179,** 2356-2360.

(83) M. Zhao, H. Liao, L. Ning, Q. Zhang, Q. Liu and Z. Xia, Next-generation narrow-band green-emitting $RbLi(Li_3SiO_4)_2:Eu^{2+}$ phosphor for backlight display application, *Adv. Mater.*, 2018, **30,** 1802489.

(84) G. Li, M. Li, L. Li, H. Yu, H. Zou, L. Zou, S. Gan and X. Xu, Luminescent properties of $Sr_2Al_2SiO_7:Ce^{3+},Eu^{2+}$ phosphors for near UV-excited white light-emitting diodes, *Mater. Lett.*, 2011, **65,** 3418-3420.

(85) M.-H. Fang, Leaño, Jr. J. L. and R.-S. Liu, Control of narrow-band emission in phosphor materials

for application in light-emitting diodes, *ACS Energy Lett.*, 2018, **3,** 2573-2586.

(86) D. Dutczak, T. Jüstel, C. Ronda and A. Meijerink, Eu^{2+} luminescence in strontium aluminates, *Phys. Chem. Chem. Phys.*, 2015, **17,** 15236-15249.

(87-1) C. B. Palan, N. S. Bajaj and S. K. Omanwar, Luminescence properties of Eu^{2+} doped SrB_4O_7 phosphor for radiation dosimetry, *Mater. Res. Bull.*, 2016, **76,** 216-221.

(87-2) A. Perloff and S. Block, The crystal structure of the strontium and lead tetraborates, SrO. $2B_2O_3$ and $PbO.2B_2O_3$, *Acta Cryst.*, 1981, **20,** 274-279.

(88) D. Cao, H. Wang, H. Wei and W. Yang, Preparation, electronic structure, and photoluminescent properties of Eu^{2+} activated $BaSi_2O_5$ powder phosphors for solid-state lighting, *J. Semicond.*, 2015, **36,** 123008.

(89) M. Derbel, A. Mbarek and M. Fourati, Photoluminescence properties of $CdSrP_2O_7:Eu^{2+}$ blue phosphor for white LED applications, *Optik*, 2016, **127,** 5870-5875.

(90) Z. Yang, D. Xu, J. Du, X. Gao and J. Sun, Tunable luminescence and energy transfer of a Eu^{2+}/Mn^{2+} co-doped $Sr_3Na_Y(PO_4)_3F$ phosphor for white LEDs, *RSC Adv.*, 2016, **6,** 87493-87501.

(91) H. Kang, K. N. Lee, S. Unithrattil, H. J. Kim, J. H. Oh, J. S. Yoo, W. B. Im and Y. R. Do, Narrow-band $SrMgAl_{10}O_{17}:Eu^{2+},Mn^{2+}$ green phosphors for wide-color-gamut backlight for LCD displays, *ACS Omega*, 2020, **5,** 19516-19524.